Numerische Mathematik (2022) 150:803–847
https://doi.org/10.1007/s00211-022-01269-0

Numerische Mathematik

Spectral Galerkin boundary element methods for high-frequency sound-hard scattering problems

Fatih Ecevit[1] · Yassine Boubendir[2] · Akash Anand[3] · Souaad Lazergui[2]

Received: 13 November 2020 / Revised: 1 January 2022 / Accepted: 15 January 2022 /
Published online: 11 February 2022

Abstract

This paper is concerned with the design of two different classes of Galerkin boundary element methods for the solution of high-frequency sound-hard scattering problems in the exterior of two-dimensional smooth convex scatterers. We prove in this paper that both methods require a small increase (in the order of k^ϵ for any $\epsilon > 0$) in the number of degrees of freedom to guarantee frequency independent precisions with increasing wavenumber k. In addition, the accuracy of the numerical solutions are independent of frequency provided sufficiently many terms in the asymptotic expansion are incorporated into the integral equation formulation. Numerical results validating $\mathcal{O}(k^\epsilon)$ algorithms are presented.

Keywords High-frequency scattering · Integral equations · Frequency independent solutions

F. Ecevit is supported by the Scientific and Technological Research Council of Turkey through grant TÜBİTAK-1001-117F056. Y. Boubendir's work was supported by the NSF through Grants DMS-1720014 and DMS-2011843. A. Anand gratefully acknowledges the support by Science & Engineering Research Board through File No MTR/2017/000643.

✉ Fatih Ecevit
fatih.ecevit@boun.edu.tr

Yassine Boubendir
boubendi@njit.edu

Akash Anand
akasha@iitk.ac.in

Souaad Lazergui
sl584@njit.edu

[1] Department of Mathematics, Boğaziçi University, Bebek TR 34342 Istanbul, Turkey

[2] Department of Mathematical Sciences, New Jersey Institute of Technology, University Heights, Newark, NJ 07102, USA

[3] Department of Mathematics and Statistics, Indian Institute of Technology Kanpur, 327 Faculty Building, Kanpur, UP 208016, India

Mathematics Subject Classification 65N38 · 78M35 · 35P25 · 65N12

1 Introduction

Wave propagation simulations at high frequencies require appropriate design of numerical methods. Generally speaking, classical approaches based on finite elements [5, 22, 34], integral equations [2, 4, 8, 11, 50], and finite differences [46, 48, 49] demand discretization in the order of the wavelength which produce very large linear systems for high wavenumbers. Therefore they are not suitable in the high frequency regime because of the required computational cost. This is the main reason why several research projects geared towards the design and analysis of high-frequency simulation strategies were initiated. For instance, in the case of sound-soft scattering problems, several methods were introduced in the context of single and multiple scattering configurations [7, 9, 10, 23–26, 31, 38]. Most of these methods were materialized thanks to the high-frequency asymptotic expansion (ansatz) of the normal derivative of the total field, derived by Melrose and Taylor in the well known paper [45], for the Dirichlet boundary value problem. Using the asymptotic expansion of the total field corresponding to the Neumann problem, also given in the paper [45], here we propose new high-frequency Galerkin boundary methods for sound-hard scattering problems for smooth convex obstacles.

For the Dirichlet boundary value problem, most of the aforementioned techniques use the Melrose–Taylor ansatz. These include the localized integration based Nyström scheme proposed for single [9, 10] and multiple scattering problems [7] (for the derivation of multiple scattering ansatz see [3, 27]), collocation technique depending on the numerical steepest descent method [38], and the Galerkin boundary element methods [23, 25, 26]. The algorithms developed in [7, 9, 10, 38] are not supported with convergence analyses, and those in [7, 9, 10, 23, 38] approximate the solution by zero in the deep shadow region which, as is well known, is true only in the high-frequency limit. In the case of the Dirichlet problem, this approximation does not effectively impair the accuracy of the numerical solution as it rapidly decays with increasing wavenumber in that region. However, numerical simulations show that the solution related to the Neumann case decays comparatively slower than the one for the Dirichlet problem (see Figs. 1 and 2), and therefore they may also loose accuracy for moderate frequencies. The Galerkin boundary element methods proposed in [25, 26] address this problem. For both algorithms, an increase of $\mathcal{O}(k^{\epsilon})$ (for any $\epsilon > 0$) in the number of degrees of freedom is sufficient to fix the approximation error with increasing wavenumber k.

In the last decades substantial interest has grown towards high-frequency problems in the fields of mathematical and numerical analysis [13, 14, 16–19, 23, 25, 26, 32, 33, 35–38, 40]. Indeed, as emphasized above, the design of numerical methods for these problems is based on the use of the ansatz directly in the numerical scheme. This ansatz, derived analytically using several mathematical tools such as pseudo-differential operators and asymptotic analysis, has a complicated form. This gives rise to challenging difficulties mainly related to the development of stable and convergent numerical algorithms. The aim of this paper is the design and analysis of new Galerkin

boundary element methods for the solution of high-frequency sound-hard scattering problems. From an analytical point of view, this requires a careful analysis of the Melrose-Taylor ansatz for the Neumann boundary value problem which is significantly more complicated than its Dirichlet counterpart. The derivation of the latter is provided in complete detail in [45] which is not the case for the Neumann problem. Therefore, for the sake of our analysis, here in this paper we complete the missing parts in this derivation, and also explain how the ansatz extends over the entire boundary of the scatterers.

The design and numerical analysis of the Galerkin boundary element methods proposed in this paper are based on a careful analysis of the asymptotic properties of the unknown total field η posed on the boundary of the scattering obstacle. More precisely, assuming a plane wave incidence with direction α, the design and numerical analysis of high frequency methods is reduced to the study of the asymptotic expansion (ansatz) provided by Melrose and Taylor [45]

$$\eta^{\text{slow}}(\alpha, x, k) \sim \sum_{\substack{p,q,r\geq 0\\ \ell\leq -1}} a_{p,q,r,\ell}(\alpha, x, k) \tag{1}$$

where $\eta^{\text{slow}}(\alpha, x, k) = e^{-ik\alpha\cdot x}\,\eta(\alpha, x, k)$ (see Theorems 1 and 8 below). In that connection, we first determine the Hörmander classes and obtain wavenumber explicit estimates on the derivatives of the terms $a_{p,q,r,\ell}$. Then, with the aid of this analysis, we derive sharp wavenumber explicit estimates on the derivatives of the envelope η^{slow}. Finally, we use these estimates in the optimal design and numerical analysis of two different classes Galerkin boundary element methods. As we will show, these methods are capable of delivering prescribed accuracies with the utilization of numbers of degrees of freedom that need to increase in the order of k^{ϵ} (for any $\epsilon > 0$) with increasing wavenumber, and are therefore *almost* frequency independent.

It is proved in this paper that if an adequate number of terms $a_{p,q,r,\ell}$ in the ansatz is explicitly known, then the methods designed here are frequency independent. Currently, however, these coefficients are not explicitly known, and therefore the numerical implementations presented here in this paper demand an $\mathcal{O}(k^{\epsilon})$ increase in the number of degrees of freedom to maintain accuracy with increasing k. In this connection, let us mention that the error estimates for the Galerkin boundary element methods developed for the Dirichlet [23, 25, 26] and the Neumann problem in this paper use Céa's lemma [12] which leads to an important factor expressed as a function of the wavenumber. In the Dirichlet case, this factor was shown to be $\mathcal{O}(k^{\frac{1}{3}})$ as $k \to \infty$ for the combined field and star combined integral equations [29, 30] (see also [24, 25]), and therefore the Galerkin approximations are bound to degrade with increasing frequency; this problem was addressed in [24] where, in the context of the combined field and star combined integral equations, it is shown that incorporation of the leading order term in the Dirichlet ansatz is sufficient to render the methods [25, 26] frequency independent. As we will see, the same approach applied to the Neumann problem will lead to similar observations and results.

In the context of the sound hard scattering problems considered in this paper, a coercive formulation for planar screens was developed in [15]. Moreover, for the problem

of scattering by smooth convex obstacles considered herein, a coercive formulation in indirect form was proposed in [6]. These suggest that this kind of formulation can also be derived in direct form for scattering from smooth obstacles. Assuming the existence of such formulations, we rigorously determine the minimal number of terms in the Neumann ansatz (1) that must be incorporated into the integral equation in order to cancel the effect of the aforementioned factor when Céa's lemma is used. To achieve this, we show the existence of an increasing sequence $\{\mathcal{F}_\beta\}_{\beta\geq 0}$ of finite sets of indices (p, q, r, ℓ) such that if

$$\sigma_\beta^{\text{slow}} := \sum_{(p,q,r,\ell)\in\mathcal{F}_\beta} a_{p,q,r,\ell} \tag{2}$$

is known, then the wavenumber explicit estimates on the derivatives of all orders of the new unknown

$$\rho_\beta^{\text{slow}} := \eta^{\text{slow}} - \sigma_\beta^{\text{slow}} \tag{3}$$

grow the slowest (with respect to the choice of the sets $\mathcal{F}_\beta$) as a function of k with increasing k; see Remark 2, Theorems 2 and 3. Following this, we design two numerical methods, namely the *frequency-adapted β-asymptotic Galerkin boundary element method* and the *β-asymptotic Galerkin boundary element method based on frequency dependent changes of variables*, that incorporate the "*β-asymptotic*" term $\sigma_\beta^{\text{slow}}$ (2) into any given appropriate integral equation formulation and thereby improve the error estimates by the factor $k^{-\beta/3}$. Let us note that $\beta = 0$ corresponds to the case, as at present, where no term $a_{p,q,r,\ell}$ in the ansatz (1) is explicitly known. In this case, $\mathcal{F}_0 = \varnothing$ and we use the convention that an empty sum is zero so that $\rho_0^{\text{slow}} = \eta^{\text{slow}}$.

Although the numerical methods we develop in this paper use the same constructions as in their sound-soft versions proposed in [26] and [25] respectively (see also [24]), the analyses are significantly different. The former method resolves the boundary layers around the shadow boundaries by adequate utilization of subregions in these regions with respect to the frequency. On each subregion, the method uses algebraic polynomials weighted by the oscillations in the incident field of radiation as in the Dirichlet case [26]. Similarly, as in [25], the latter method utilizes frequency dependent changes of variables to resolve the boundary layers around the shadow boundaries. In addition, we show that, for $\beta = 0$ (which means no term $a_{p,q,r,\ell}$ in the ansatz is incorporated into the integral equation formulation) both methods require only a small increase (of size $\mathcal{O}(k^\epsilon)$ for any $\epsilon > 0$) in the number of degrees of freedom to maintain accuracy with increasing k. Moreover, as mentioned above, we demonstrate that the methods are frequency independent when sufficiently many terms in the ansatz are appropriately used in the integral equation formulations.

The paper is organized as follows. In Sect. 2, we introduce the sound-hard scattering problem, and discuss the similarities and differences between the Neumann and Dirichlet high-frequency solutions. In Sect. 3, we determine the Hörmander classes of the terms $a_{p,q,r,\ell}$ in the ansatz (1) and the envelopes ρ_β^{slow} in (3), and derive sharp wavenumber dependent estimates on their derivatives. We use these estimates in the construction and numerical analysis of the *frequency-adapted β-asymptotic Galerkin*

boundary element method and the *β-asymptotic Galerkin boundary element method based on frequency dependent changes of variables* in Sect. 4. We present numerical results confirming our theoretical findings in Sect. 5. Finally, the derivation of the ansatz is presented in Appendix 1 where we also show how it extends to the entire boundary of the scatterers.

2 Problem statement

We consider the sound-hard scattering problem in the exterior of a smooth, compact and strictly convex obstacle $K \subset \mathbb{R}^2$ illuminated by a plane wave incidence $u^{\text{inc}}(x) = e^{ik\alpha\cdot x}$ with direction α, $|\alpha| = 1$ and $k > 0$. The unknown scattered field u satisfies [14, 20]

$$\begin{cases} (\Delta + k^2)u = 0 & \text{in } \mathbb{R}^2\backslash K, \\ \partial_\nu u = -\partial_\nu u^{\text{inc}} & \text{on } \partial K, \\ \lim_{r\to\infty} \sqrt{r}\left(\frac{\partial u}{\partial r} - iku\right) = 0, & r = |x|, \end{cases} \tag{4}$$

where ν is the exterior unit normal to ∂K.

The direct approach in high-frequency integral equation formulations transforms the scattering problem (4) into the computation of the (unknown) total field $\eta := u + u^{\text{inc}}$ on ∂K. Indeed, as a radiating solution to the Helmholz equation, the scattered field satisfies [14, 20]

$$u(\alpha, x, k) = \int_{\partial K} \left(\frac{\partial G_k(x, y)}{\partial \nu(y)}\, u(\alpha, y, k) - \frac{\partial u(\alpha, y, k)}{\partial \nu(y)}\, G_k(x, y) \right) ds(y) \tag{5}$$

for all x in the exterior region $\mathbb{R}^2 \setminus K$, where

$$G_k(x, y) = \frac{i}{4} H_0^{(1)}(k|x - y|)$$

is the outgoing Green's function for the Helmholtz equation and $H_0^{(1)}$ is the Hankel function of the first kind and of order zero. Moreover, Green's theorem applied to u^{inc} and $G_k(x, \cdot)$ gives, in the exterior region,

$$0 = \int_{\partial K} \left(\frac{\partial G_k(x, y)}{\partial \nu(y)}\, u^{\text{inc}}(\alpha, y, k) - \frac{\partial u^{\text{inc}}(\alpha, y, k)}{\partial \nu(y)}\, G_k(x, y) \right) ds(y). \tag{6}$$

Adding (5) and (6) and using the Neumann boundary condition $\partial_\nu u = -\partial_\nu u^{\text{inc}}$ shows that the scattered field can be expressed as the double-layer potential

$$u(\alpha, x, k) = \int_{\partial K} \frac{\partial G_k(x, y)}{\partial \nu(y)}\, \eta(\alpha, y, k)\, ds(y). \tag{7}$$

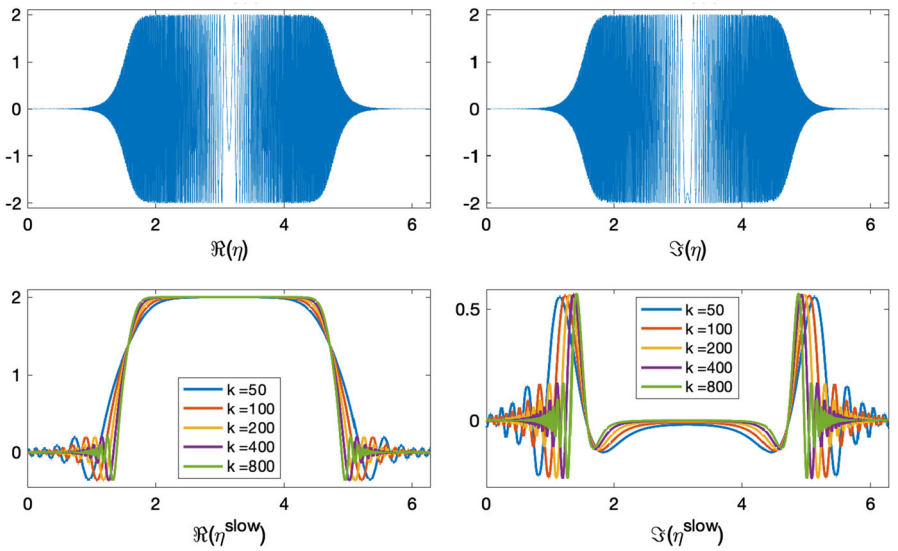

Fig. 1 Plots of the real and imaginary parts of the total field (top row) and the slow envelope (bottom row) for the sound-hard scattering problem in the case of a plane wave incidence with direction $\alpha = (1, 0)$ impinging on the unit circle $(\cos t, \sin t)$ for $k = 50, 100, 200, 400, 800$

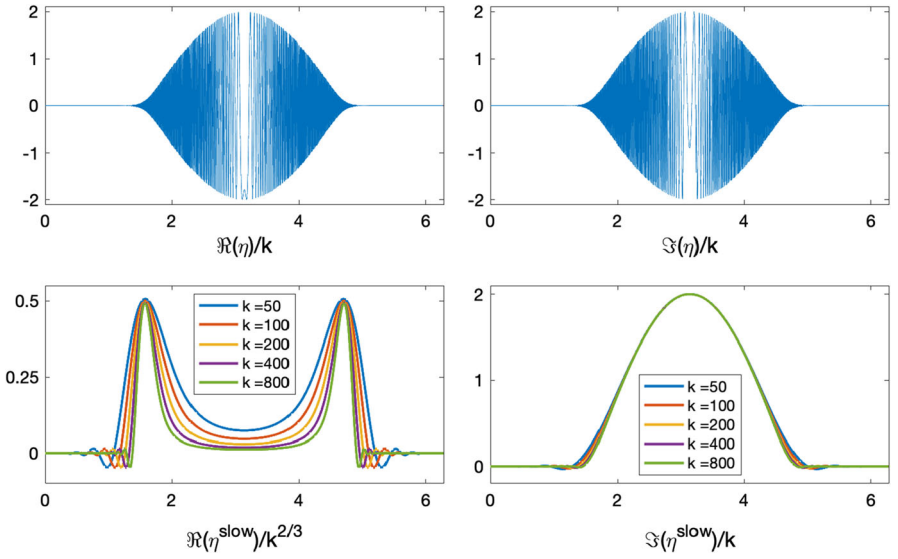

Fig. 2 Plots of the real and imaginary parts of the normal derivative of the total field modulated by k (top row) and the slow envelope modulated by $k^{2/3}$ and k (bottom row) for the sound-soft scattering problem in the case of a plane wave incidence with direction $\alpha = (1, 0)$ impinging on the unit circle $(\cos t, \sin t)$ for $k = 50, 100, 200, 400, 800$

One of the primary motivations for using direct formulations is the observation that η is amenable to phase extraction

$$\eta(\alpha, x, k) = e^{ik\alpha\cdot x}\, \eta^{\text{slow}}(\alpha, x, k) \tag{8}$$

as it is the case for the Dirichlet boundary value problem where the unknown represents the normal derivative of the total field (see Figs. 1 and 2). In this paper, we develop efficient Galerkin boundary element methods by using the asymptotic behavior (as $k \to \infty$) of the envelope η^{slow} in the construction of Galerkin approximation spaces. This approach is similar to the one used for the sound-soft scattering problem. In Figs. 1 and 2, we display the total field and the normal derivative of the total field respectively for the Neumann and Dirichlet boundary value problems. As we can see, these densities have similar asymptotic characteristics. Specifically, they both posses boundary layers around the shadow boundaries, and decay rapidly in the deep shadow region with increasing wavenumber. From a numerical perspective, however, approximating the density related to the Neumann problem is more challenging since its slow part (η^{slow}) oscillates more strongly around the shadow boundaries and decays indubitably slower in the shadow region as displayed in the simulations in Figs. 1 and 2. Consequently, obtaining highly accurate numerical approximations to the Neumann problem is significantly more challenging when compared to the Dirichlet case.

3 Hörmander classes and wavenumber explicit derivative estimates

This section is dedicated to the study of the asymptotic expansion of the envelope η^{slow} defined in (8). We first observe that the incident plane wave $u^{\text{inc}}(x) = e^{ik\alpha\cdot x}$ determines the illuminated and shadow regions, and the shadow boundaries on ∂K as

$$\begin{aligned}
\partial K^{IL} &= \{x \in \partial K : \alpha \cdot \nu(x) < 0\} \\
\partial K^{SR} &= \{x \in \partial K : \alpha \cdot \nu(x) > 0\} \\
\partial K^{SB} &= \{x \in \partial K : \alpha \cdot \nu(x) = 0\}.
\end{aligned}$$

We let $2P = |\partial K|$, and we choose γ as the $2P$-periodic arc length parameterization of the boundary ∂K in the counterclockwise direction such that the shadow boundaries $\partial K^{SB} = \gamma(\{t_1, t_2\})$ are determined by the parameters $0 < t_1 < t_2 < 2P$ satisfying $t_1 + t_2 = 2P$, and the illuminated and shadow regions are given by $\partial K^{IL} = \gamma((t_1, t_2))$ and $= \partial K^{SR} = \gamma((0, t_1) \cup (t_2, 2P))$. In what follows we shall write ∂K^{SB} for $\{t_1, t_2\}$, ∂K^{IL} for (t_1, t_2), and ∂K^{SR} for $(0, t_1) \cup (t_2, 2P)$. For convenience, we shall also write $\eta(s, k)$, $\eta^{\text{slow}}(s, k)$, $\nu(s)$, etc. rather than $\eta(\alpha, \gamma(s), k)$, $\eta^{\text{slow}}(\alpha, \gamma(s), k)$, $\nu(\gamma(s))$, etc. where α is eliminated and $\gamma(s)$ is replaced by s. In the next theorem, we present the asymptotic behavior of η^{slow} in a two-dimensional setting while a general version is given in Theorem 8 of Appendix 1.

Theorem 1 *The envelope η^{slow} belongs to the Hörmander class $S^0_{\frac{2}{3},\frac{1}{3}}([0, 2P] \times (0, \infty))$ and admits the asymptotic expansion*

$$\eta^{\mathrm{slow}}(s,k) \sim \sum_{\substack{p,q,r\in\mathbb{Z}_+\\ \ell\in-\mathbb{N}}} a_{p,q,r,\ell}(s,k) \tag{9}$$

with

$$a_{p,q,r,\ell}(s,k) = k^{-\frac{1+2p+3q+r+\ell}{3}+(\ell+1)_-}\, b_{p,q,r,\ell}(s)\, (\Psi^{r,\ell})^{(p)}(k^{\frac{1}{3}} Z(s)) \tag{10}$$

where $\mathbb{Z}_+$ is the set of non-negative integers, $t_- = \min\{t,0\}$, $b_{p,q,r,\ell}$ are $2P$-periodic complex-valued C^∞ functions, Z is a $2P$-periodic real-valued C^∞ function that is positive on the illuminated region ∂K^{IL}, negative on the shadow region ∂K^{SR}, and vanishes precisely to first order at the shadow boundary ∂K^{SR}. Finally $\Psi^{r,\ell}$ are complex-valued C^∞ functions which admit the asymptotic expansions

$$\Psi^{r,\ell}(\tau) \sim \sum_{j\in\mathbb{Z}_+} \alpha_{r,\ell,j}\, \tau^{1+\ell-2r-3j} \qquad \text{as } \tau \to +\infty$$

and rapidly decrease in the sense of Schwarz as $\tau \to -\infty$.

For concise definitions of Hörmander classes and asymptotic expansions we refer to [27,§2.2].

In this section, we study the asymptotic behavior of the terms $a_{p,q,r,\ell}$ appearing in the expansion (9), and first show that they belong to the Hörmander class $S^{\vartheta(p,q,r,\ell)}_{\frac{2}{3},\frac{1}{3}}([0,2P]\times(0,\infty))$ where

$$\begin{aligned}\vartheta(p,q,r,\ell) := &-\frac{1+2p+3q+r+\ell}{3}\\ &+(\ell+1)_- + \begin{cases} 0, & 1+\ell-2r-p<0,\\ \frac{1+\ell-2r-p}{3}, & 1+\ell-2r-p\geq 0.\end{cases}\end{aligned} \tag{11}$$

We then use this result to carry out a similar study for the expressions $\rho^{\mathrm{slow}}_\beta$ which we now define.

Definition 1 Given $\beta\in\mathbb{Z}_+$, we define

$$\sigma^{\mathrm{slow}}_\beta := \sum_{(p,q,r,\ell)\in\mathcal{F}_\beta} a_{p,q,r,\ell} \qquad \text{and} \qquad \rho^{\mathrm{slow}}_\beta := \eta^{\mathrm{slow}} - \sigma^{\mathrm{slow}}_\beta \tag{12}$$

where

$$\mathcal{F}_\beta := \left\{(p,q,r,\ell)\in\mathbb{Z}_+\times\mathbb{Z}_+\times\mathbb{Z}_+\times(-\mathbb{N}) : \vartheta(p,q,r,\ell) > -\frac{\beta}{3}\right\}. \tag{13}$$

We also set

$$\sigma_\beta := e^{ik\,\alpha\cdot\gamma}\sigma^{\mathrm{slow}}_\beta \qquad \text{and} \qquad \rho_\beta := \eta - \sigma_\beta = e^{ik\,\alpha\cdot\gamma}\rho^{\mathrm{slow}}_\beta. \tag{14}$$

Throughout the text, we use the standard convention that an empty sum is zero. In particular (since $\vartheta(p,q,r,\ell) \leq 0$ for any $(p,q,r,\ell) \in \mathbb{Z}_+ \times \mathbb{Z}_+ \times \mathbb{Z}_+ \times (-\mathbb{N})$) $\mathcal{F}_0 = \varnothing$ so that $\sigma_0^{\text{slow}} = 0$ and $\sigma_0 = 0$, and therefore $\rho_0^{\text{slow}} = \eta^{\text{slow}}$ and $\rho_0 = \eta$.

As mentioned in the introduction, the use of Céa's lemma gives rise to a factor depending on the wavenumber which effectively means the need for higher number of degrees freedom with increasing k. The goal of the previous definition is to eliminate this factor by incorporating sufficiently many terms in the asymptotic expansion into any given continuous and coercive integral equation formulation. Indeed, as shown in the following analysis, the definition of $\sigma_\beta^{\text{slow}}$ (12) is optimal in the sense that it leads to the balancing factor $k^{-\beta/3}$ subject to a minimum number of terms $a_{p,q,r,\ell}$ incorporated into the integral equation (see Remark 2, and Theorems 2 and 3). This represents a very important step in the design of Galerkin approximation spaces which can provide prescribed error tolerances with the utilization of frequency independent numbers of degrees of freedom.

Let us begin our analysis by giving the following result which is immediate from the asymptotic behavior of $\Psi^{r,\ell}$ described in Theorem 1.

Lemma 1 *For all $p, r \in \mathbb{Z}_+$ and $\ell \in \mathbb{Z}$, there exists a positive constant C such that*

$$|(\Psi^{r,\ell})^{(p)}(\tau)| \leq C \begin{cases} (1+|\tau|)^{\gamma_{r,\ell}-p}, & \text{if } p > 1+\ell-2r \geq 0, \\ (1+|\tau|)^{1+\ell-2r-p}, & \text{otherwise}, \end{cases} \tag{15}$$

holds for all $\tau \in \mathbb{R}$ where

$$1+\ell-2r \equiv \gamma_{r,\ell} \mod 3 \quad \text{with} \quad \gamma_{r,\ell} \in \{-3,-2,-1\}.$$

Remark 1 In the rest of the paper, the notation $A \lesssim B$ will mean $0 \leq A \leq cB$ for the range of values of the wavenumber k relevant to the context where c is a positive constant independent of k (which might, however, depend on the geometry of the scattering obstacle, the direction of incidence, and all the other parameters in the context). Additionally, the notation $A \asymp B$ will mean $A \lesssim B$ and $B \lesssim A$.

With the aid of Theorem 1, Lemma 1, and Lemma 8 in Appendix 1, we now characterize the Hörmander classes of $a_{p,q,r,\ell}$ and derive wavenumber explicit estimates on their derivatives.

Lemma 2 [Hörmander classes of $a_{p,q,r,\ell}$] *For any $p, q, r \in \mathbb{Z}_+$ and $\ell \in \mathbb{Z}$, $a_{p,q,r,\ell}$ belongs to the Hörmander class $S^{\vartheta(p,q,r,\ell)}_{\frac{2}{3},\frac{1}{3}}([0,2P]\times(0,\infty))$.*

Proof Given $n, m, p, q, r \in \mathbb{Z}_+$ and $\ell \in \mathbb{Z}$, an application of Lemma 8 to $a_{p,q,r,\ell}$ (10) entails

$$\begin{aligned} |D_s^n D_k^m a_{p,q,r,\ell}(s,k)| &\lesssim k^{-\frac{1+2p+3q+r+\ell}{3}+(\ell+1)_- - m} \\ &\times \sum_{0\leq j\leq n+m} k^{\frac{j}{3}} |(\Psi^{r,\ell})^{(p+j)}(k^{\frac{1}{3}} Z(s))| \end{aligned} \tag{16}$$

for all $(s,k) \in [0,2P]\times(0,\infty)$.

When $1+\ell-2r<0$, use of (15) in (16) implies

$$\begin{aligned}|D_s^n D_k^m\, a_{p,q,r,\ell}(s,k)| &\lesssim k^{-\frac{1+2p+3q+r+\ell}{3}+(\ell+1)_- -m}\\ &\quad\times \sum_{0\le j\le n+m} k^{\frac{j}{3}}(1+k^{\frac{1}{3}}|Z(s)|)^{1+\ell-2r-p-j}\\ &\lesssim k^{-\frac{1+2p+3q+r+\ell}{3}+(\ell+1)_- -m}\sum_{0\le j\le n+m} k^{\frac{j}{3}}\\ &\lesssim k^{-\frac{1+2p+3q+r+\ell}{3}+(\ell+1)_- +\frac{n}{3}-\frac{2m}{3}}\end{aligned}$$

and this, in turn, implies that $a_{p,q,r,l}\in S^{\vartheta(p,q,r,\ell)}_{\frac{2}{3},\frac{1}{3}}([0,2P]\times(0,\infty))$.

When $1+\ell-2r\ge 0$, use of (15) in (16) gives

$$\begin{aligned}|D_s^n D_k^m\, a_{p,q,r,\ell}(s,k)| &\lesssim k^{-\frac{1+2p+3q+r+\ell}{3}+(\ell+1)_- -m}\\ &\quad\times\Bigg\{\sum_{\substack{0\le j\le n+m\\ j\le 1+\ell-2r-p}} k^{\frac{j}{3}}(1+k^{\frac{1}{3}}|Z(s)|)^{1+\ell-2r-p-j}\\ &\quad+\sum_{\substack{0\le j\le n+m\\ j>1+\ell-2r-p}} k^{\frac{j}{3}}(1+k^{\frac{1}{3}}|Z(s)|)^{\gamma_{r,\ell}-p-j}\Bigg\}.\end{aligned}\tag{17}$$

If $1+\ell-2r-p<0$, (17) reduces to

$$\begin{aligned}|D_s^n D_k^m\, a_{p,q,r,\ell}(s,k)| &\lesssim k^{-\frac{1+2p+3q+r+\ell}{3}+(\ell+1)_- -m}\\ &\quad\times\sum_{0\le j\le n+m} k^{\frac{j}{3}}(1+k^{\frac{1}{3}}|Z(s)|)^{\gamma_{r,\ell}-p-j}\\ &\lesssim k^{-\frac{1+2p+3q+r+\ell}{3}+(\ell+1)_- -m}\sum_{0\le j\le n+m} k^{\frac{j}{3}}\\ &\lesssim k^{-\frac{1+2p+3q+r+\ell}{3}+(\ell+1)_- -m}\,k^{\frac{n+m}{3}}\\ &\lesssim k^{-\frac{1+2p+3q+r+\ell}{3}+(\ell+1)_- +\frac{n}{3}-\frac{2m}{3}}\\ &\lesssim k^{\vartheta(p,q,r,\ell)+\frac{n}{3}-\frac{2m}{3}}\end{aligned}$$

so that $a_{p,q,r,l}\in S^{\vartheta(p,q,r,\ell)}_{\frac{2}{3},\frac{1}{3}}([0,2P]\times(0,\infty))$. If $1+\ell-2r-p\ge 0$, setting $J=\min\{n+m,1+\ell-2r-p\}$, (17) takes on the form

$$\begin{aligned}&|D_s^n D_k^m\, a_{p,q,r,\ell}(s,k)|\\ &\lesssim k^{-\frac{1+2p+3q+r+\ell}{3}+(\ell+1)_- -m}\Bigg\{\sum_{0\le j\le J} k^{\frac{j}{3}}(1+k^{\frac{1}{3}}|Z(s)|)^{1+\ell-2r-p-j}\end{aligned}$$

$$
\begin{aligned}
&+ \sum_{J<j\le n+m} k^{\frac{j}{3}}(1+k^{\frac{1}{3}}|Z(s)|)^{\gamma_{r,\ell}-p-j}\Big\}\\
&\lesssim k^{-\frac{1+2p+3q+r+\ell}{3}+(\ell+1)_- -m}\Big\{\sum_{0\le j\le J} k^{\frac{j}{3}}k^{\frac{1+\ell-2r-p-j}{3}} + \sum_{J<j\le n+m} k^{\frac{j}{3}}\Big\}\\
&\lesssim k^{-\frac{1+2p+3q+r+\ell}{3}+(\ell+1)_- -m}\Big\{k^{\frac{1+\ell-2r-p}{3}} + \sum_{J<j\le n+m} k^{\frac{j}{3}}\Big\}.
\end{aligned}
$$

This entails, when $0 \le 1+\ell-2r-p < n+m$

$$
\begin{aligned}
|D_s^n D_k^m\, a_{p,q,r,\ell}(s,k)| &\lesssim k^{-\frac{1+2p+3q+r+\ell}{3}+(\ell+1)_- -m}\left\{k^{\frac{1+\ell-2r-p}{3}} + k^{\frac{n+m}{3}}\right\}\\
&\lesssim k^{-\frac{1+2p+3q+r+\ell}{3}+(\ell+1)_- -m}\, k^{\frac{n+m}{3}}\\
&\lesssim k^{-\frac{1+2p+3q+r+\ell}{3}+(\ell+1)_- +\frac{n}{3}-\frac{2m}{3}}\\
&\lesssim k^{\vartheta(p,q,r,\ell)+\frac{n}{3}-\frac{2m}{3}},
\end{aligned}
$$

and when $n+m \le 1+\ell-2r-p$

$$
\begin{aligned}
|D_s^n D_k^m\, a_{p,q,r,\ell}(s,k)| &\lesssim k^{-\frac{1+2p+3q+r+\ell}{3}+(\ell+1)_- -m}k^{\frac{1+\ell-2r-p}{3}}\\
&\lesssim k^{\vartheta(p,q,r,\ell)-m} \lesssim k^{\vartheta(p,q,r,\ell)+\frac{n}{3}-\frac{2m}{3}}.
\end{aligned}
$$

These show that $a_{p,q,r,l} \in S^{\vartheta(p,q,r,\ell)}_{\frac{2}{3},\frac{1}{3}}([0,2P]\times(0,\infty))$ when $1+\ell-2r-p \ge 0$. Therefore the proof is complete. □

For the developments that follow, we define

$$
W(s,k) := k^{-\frac{1}{3}} + |\omega(s)| \quad \text{with} \quad \omega(s) := (s-t_1)(t_2-s) \tag{18}
$$

for any $k > 0$.

Lemma 3 (Wavenumber explicit estimates on the derivatives of $a_{p,q,r,\ell}$) *Given $k_0 > 0$ and $n, p, q, r \in \mathbb{Z}_+$ and $\ell \in \mathbb{Z}$, the estimate*

$$
|D_s^n a_{p,q,r,\ell}(s,k)| \lesssim k^{-\frac{1+2p+3q+r+\ell}{3}+(\ell+1)_-} \times \begin{cases} \sum_{0\le j\le n} W(s,k)^{-j}, & 1+\ell-2r-p<0,\\ \lambda_{p,r,\ell,n}(s,k), & 1+\ell-2r-p\ge 0, \end{cases} \tag{19}
$$

holds for all $(s,k) \in [0,2P]\times[k_0,\infty)$ where

$$
\lambda_{p,r,\ell,n}(s,k) := k^{\frac{1+\ell-2r-p}{3}} + \sum_{1+\ell-2r-p<j\le n} W(s,k)^{-j}.
$$

Proof Given $n, p, q, r \in \mathbb{Z}_+$ and $\ell \in \mathbb{Z}$, use of Lemma 8 entails for the derivatives of $a_{p,q,r,\ell}$ (10)

$$|D_s^n\, a_{p,q,r,\ell}(s,k)| \lesssim k^{-\frac{1+2p+3q+r+\ell}{3}+(\ell+1)_-} \sum_{0\le j\le n} k^{\frac{j}{3}} |(\Psi^{r,\ell})^{(p+j)}(k^{\frac{1}{3}} Z(s))| \quad (20)$$

for all $(s,k) \in [0, 2P] \times (0,\infty)$.

When $1+\ell-2r < 0$, use of (15) in (20) implies

$$\begin{aligned}
|D_s^n\, a_{p,q,r,\ell}(s,k)| &\lesssim k^{-\frac{1+2p+3q+r+\ell}{3}+(\ell+1)_-} \sum_{0\le j\le n} k^{\frac{j}{3}} (1+k^{\frac{1}{3}}|Z(s)|)^{1+\ell-2r-p-j} \\
&\lesssim k^{-\frac{1+2p+3q+r+\ell}{3}+(\ell+1)_-} \sum_{0\le j\le n} k^{\frac{j}{3}} (1+k^{\frac{1}{3}}|\omega(s)|)^{1+\ell-2r-p-j} \\
&\lesssim k^{-\frac{1+2p+3q+r+\ell}{3}+(\ell+1)_-} \sum_{0\le j\le n} k^{\frac{j}{3}} (1+k^{\frac{1}{3}}|\omega(s)|)^{-j} \\
&\lesssim k^{-\frac{1+2p+3q+r+\ell}{3}+(\ell+1)_-} \sum_{0\le j\le n} (k^{-\frac{1}{3}}+|\omega(s)|)^{-j}.
\end{aligned}$$

When $1+\ell-2r \ge 0$, use of (15) in (20) gives

$$\begin{aligned}
&|D_s^n\, a_{p,q,r,\ell}(s,k)| \\
&\lesssim k^{-\frac{1+2p+3q+r+\ell}{3}+(\ell+1)_-} \Bigg\{ \sum_{\substack{0\le j\le n \\ j\le 1+\ell-2r-p}} k^{\frac{j}{3}} (1+k^{\frac{1}{3}}|Z(s)|)^{1+\ell-2r-p-j} \\
&\quad + \sum_{\substack{0\le j\le n \\ j> 1+\ell-2r-p}} k^{\frac{j}{3}} (1+k^{\frac{1}{3}}|Z(s)|)^{\gamma_{r,\ell}-p-j} \Bigg\}. \qquad (21)
\end{aligned}$$

If $1+\ell-2r-p < 0$, (21) reduces to

$$\begin{aligned}
|D_s^n\, a_{p,q,r,\ell}(s,k)| &\lesssim k^{-\frac{1+2p+3q+r+\ell}{3}+(\ell+1)_-} \sum_{0\le j\le n} k^{\frac{j}{3}} (1+k^{\frac{1}{3}}|Z(s)|)^{\gamma_{r,\ell}-p-j} \\
&\lesssim k^{-\frac{1+2p+3q+r+\ell}{3}+(\ell+1)_-} \sum_{0\le j\le n} k^{\frac{j}{3}} (1+k^{\frac{1}{3}}|Z(s)|)^{-j} \\
&\lesssim k^{-\frac{1+2p+3q+r+\ell}{3}+(\ell+1)_-} \sum_{0\le j\le n} k^{\frac{j}{3}} (1+k^{\frac{1}{3}}|\omega(s)|)^{-j} \\
&= k^{-\frac{1+2p+3q+r+\ell}{3}+(\ell+1)_-} \sum_{0\le j\le n} (k^{-\frac{1}{3}}+|\omega(s)|)^{-j}.
\end{aligned}$$

If $1+\ell-2r-p \ge 0$, setting $J = \min\{n, 1+\ell-2r-p\}$, (21) becomes

$$|D_s^n\, a_{p,q,r,\ell}(s,k)|$$

$$
\begin{aligned}
&\lesssim k^{-\frac{1+2p+3q+r+\ell}{3}+(\ell+1)_-}\Bigg\{\sum_{0\le j\le J} k^{\frac{j}{3}}(1+k^{\frac{1}{3}}|Z(s)|)^{1+\ell-2r-p-j}\\
&+\sum_{J<j\le n} k^{\frac{j}{3}}(1+k^{\frac{1}{3}}|Z(s)|)^{\gamma_{r,\ell}-p-j}\Bigg\}\\
&\lesssim k^{-\frac{1+2p+3q+r+\ell}{3}+(\ell+1)_-}\Bigg\{\sum_{0\le j\le J} k^{\frac{j}{3}}k^{\frac{1+\ell-2r-p-j}{3}}\\
&+\sum_{J<j\le n} k^{\frac{j}{3}}(1+k^{\frac{1}{3}}|\omega(s)|)^{\gamma_{r,\ell}-p-j}\Bigg\}\\
&\lesssim k^{-\frac{1+2p+3q+r+\ell}{3}+(\ell+1)_-}\Big\{k^{\frac{1+\ell-2r-p}{3}}+\sum_{J<j\le n} k^{\frac{j}{3}}(1+k^{\frac{1}{3}}|\omega(s)|)^{-j}\Big\}\\
&= k^{-\frac{1+2p+3q+r+\ell}{3}+(\ell+1)_-}\Big\{k^{\frac{1+\ell-2r-p}{3}}+\sum_{j=J+1}^{n}(k^{-\frac{1}{3}}+|\omega(s)|)^{-j}\Big\}.
\end{aligned}
$$

Thus the result follows. □

Using Lemma 3, we can obtain the following.

Corollary 1 (Simplified wavenumber explicit estimates on the derivatives of $a_{p,q,r,\ell}$) *Given $k_0 > 0$ and $n, p, q, r \in \mathbb{Z}_+$ and $\ell \in \mathbb{Z}$, the estimate*

$$
|D_s^n a_{p,q,r,\ell}(s,k)| \lesssim k^{\vartheta(p,q,r,\ell)}\, W(s,k)^{-n} \tag{22}
$$

holds for all $(s,k) \in [0,2P]\times[k_0,\infty)$.

We now make use of Lemma 2 and Corollary 1 to characterize the Hörmander classes and derive wavenumber explicit estimates on the derivatives of the envelopes $\rho_{\mathcal{F}}^{\text{slow}}$ we introduce next.

Definition 2 Given a finite set $\mathcal{F} \subset \mathbb{Z}_+ \times \mathbb{Z}_+ \times \mathbb{Z}_+ \times (-\mathbb{N})$, we define

$$
\rho_{\mathcal{F}}^{\text{slow}} := \eta^{\text{slow}} - \sigma_{\mathcal{F}}^{\text{slow}}
$$

where

$$
\sigma_{\mathcal{F}}^{\text{slow}} := \sum_{(p,q,r,\ell)\in\mathcal{F}} a_{p,q,r,\ell}.
$$

We also set

$$
\vartheta(\mathcal{F}) := \max\{\vartheta(p,q,r,\ell) : (p,q,r,\ell) \in \mathbb{Z}_+ \times \mathbb{Z}_+ \times \mathbb{Z}_+ \times (-\mathbb{N})\backslash\mathcal{F}\}.
$$

Remark 2 As is apparent from (13), for any $\beta \in \mathbb{Z}_+$, the smallest finite set $\mathcal{F} \subset \mathbb{Z}_+ \times \mathbb{Z}_+ \times \mathbb{Z}_+ \times (-\mathbb{N})$ having $\vartheta(\mathcal{F}) = -\frac{\beta}{3}$ is precisely $\mathcal{F}_\beta$, and the sets $\mathcal{F}_\beta$ are increasing with increasing β. Moreover, comparing Definitions 1 and 2, we see that

$$\sigma_\beta^{\text{slow}} = \sigma_{\mathcal{F}_\beta}^{\text{slow}} \qquad \text{and} \qquad \rho_\beta^{\text{slow}} = \rho_{\mathcal{F}_\beta}^{\text{slow}}.$$

The next theorem thus clarifies the optimality of the sets $\mathcal{F}_\beta$ in connection with the wavenumber explicit derivative estimates.

Theorem 2 *Given a finite set $\mathcal{F} \subset \mathbb{Z}_+ \times \mathbb{Z}_+ \times \mathbb{Z}_+ \times (-\mathbb{N})$, the envelope $\rho_{\mathcal{F}}^{\text{slow}}$ belongs to $S^{\vartheta(\mathcal{F})}_{\frac{2}{3},\frac{1}{3}}([0,2P] \times (0,\infty))$. Moreover, given $k_0 > 1$ and $n \in \mathbb{Z}_+$, the estimate*

$$|D_s^n \rho_{\mathcal{F}}^{\text{slow}}(s,k)| \lesssim k^{\vartheta(\mathcal{F})}\, W(s,k)^{-n} \tag{23}$$

holds for all $(s,k) \in [0,2P] \times [k_0,\infty)$.

Proof First note that the definition of $\vartheta(p,q,r,\ell)$ (see (11)) implies

$$\{\vartheta(p,q,r,\ell) : (p,q,r,\ell) \in \mathbb{Z}_+ \times \mathbb{Z}_+ \times \mathbb{Z}_+ \times (-\mathbb{N})\} = -\frac{1}{3}\,\mathbb{Z}_+.$$

Thus, in light of Theorem 1 (specifically $\eta^{\text{slow}} \in S^0_{\frac{2}{3},\frac{1}{3}}$ and (9)) and Lemma 2, the definitions of Hörmander classes and asymptotic expansions (see e.g. [27,§2]) imply $\rho_{\mathcal{F}}^{\text{slow}} \in S^{\vartheta(\mathcal{F})}_{\frac{2}{3},\frac{1}{3}}$.

Given $n \in \mathbb{Z}_+$, let

$$\mathcal{F}_n := \left\{(p,q,r,\ell) \in \mathbb{Z}_+ \times \mathbb{Z}_+ \times \mathbb{Z}_+ \times (-\mathbb{N}) : \vartheta(p,q,r,\ell) \geq m(\mathcal{F}) - \frac{n}{3}\right\}$$

where

$$m(\mathcal{F}) := \min\left\{\vartheta(p,q,r,\ell) : (p,q,r,\ell) \in \mathcal{F} \cup \{(0,0,0,-1)\}\right\}.$$

Then $\mathcal{F} \subset \mathcal{F}_n$ so that

$$\sigma_{\mathcal{F}_n}^{\text{slow}} = \sigma_{\mathcal{F}}^{\text{slow}} + \sigma_{\mathcal{F}_n \setminus \mathcal{F}}^{\text{slow}},$$

and therefore

$$\rho_{\mathcal{F}}^{\text{slow}} = \rho_{\mathcal{F}_n}^{\text{slow}} + \sigma_{\mathcal{F}_n \setminus \mathcal{F}}^{\text{slow}}. \tag{24}$$

A second appeal to Theorem 1 (specifically $\eta^{\text{slow}} \in S^0_{\frac{2}{3},\frac{1}{3}}$ and (9)) and Lemma 2 implies through the definitions of Hörmander classes and asymptotic expansions that

$$\rho_{\mathcal{F}_n}^{\text{slow}} \in S^{\vartheta(\mathcal{F}_n)}_{\frac{2}{3},\frac{1}{3}}. \tag{25}$$

The very definition of $\mathcal{F}_n$ entails $\vartheta(\mathcal{F}_n) = m(\mathcal{F}) - \dfrac{n+1}{3}$ so that, by definition of Hörmander classes, (25) gives

$$|D_s^n \rho_{\mathcal{F}_n}^{\mathrm{slow}}(s,k)| \lesssim (1+k)^{m(\mathcal{F})-\frac{n+1}{3}+\frac{n}{3}} \lesssim (1+k)^{m(\mathcal{F})-\frac{1}{3}} W(s,k)^{-n}. \tag{26}$$

On the other hand, Corollary 1 yields

$$\begin{aligned} |D_s^n \rho_{\mathcal{F}_n\setminus\mathcal{F}}^{\mathrm{slow}}(s,k)| &\lesssim \sum_{(p,q,r,\ell)\in\mathcal{F}_n\setminus\mathcal{F}} k^{\vartheta(p,q,r,\ell)} W(s,k)^{-n} \\ &\lesssim k^{\max\{\vartheta(p,q,r,\ell):(p,q,r,\ell)\in\mathcal{F}_n\setminus\mathcal{F}\}} W(s,k)^{-n}. \end{aligned} \tag{27}$$

Using (26) and (27) in (24), we therefore deduce

$$\begin{aligned} |D_s^n \rho_{\mathcal{F}}^{\mathrm{slow}}(s,k)| &\lesssim \left[(1+k)^{m(\mathcal{F})-\frac{1}{3}} + k^{\max\{\vartheta(p,q,r,\ell):(p,q,r,\ell)\in\mathcal{F}_n\setminus\mathcal{F}\}}\right] W(s,k)^{-n} \\ &\lesssim k^{\max\{\vartheta(p,q,r,\ell):(p,q,r,\ell)\in\mathcal{F}_n\setminus\mathcal{F}\}} W(s,k)^{-n}. \end{aligned}$$

Accordingly, since

$$\begin{aligned} &\max\{\vartheta(p,q,r,\ell) : (p,q,r,\ell)\in\mathcal{F}_n\setminus\mathcal{F}\} \\ &\quad = \max\{\vartheta(p,q,r,\ell) : (p,q,r,\ell)\in\mathbb{Z}_+\times\mathbb{Z}_+\times\mathbb{Z}_+\times(-\mathbb{N})\setminus\mathcal{F}\} = \vartheta(\mathcal{F}), \end{aligned}$$

(23) follows. □

The design and analysis of the Galerkin boundary element methods presented in Sect. 4 are based on the following theorem which is immediate from Remark 2 and Theorem 2.

Theorem 3 *Given $\beta\in\mathbb{Z}_+$, the smallest finite set $\mathcal{F}\subset\mathbb{Z}_+\times\mathbb{Z}_+\times\mathbb{Z}_+\times(-\mathbb{N})$ having $\vartheta(\mathcal{F}) = -\frac{\beta}{3}$ is precisely $\mathcal{F}_\beta$ as defined in (13). Moreover $\rho_\beta^{\mathrm{slow}}$ (12) belongs to the Hörmander class $S^{-\frac{\beta}{3}}_{\frac{2}{3},\frac{1}{3}}([0,2P]\times(0,\infty))$ and, for any given $k_0>1$ and $n\in\mathbb{Z}_+$, the estimate*

$$|D_s^n \rho_\beta^{\mathrm{slow}}(s,k)| \lesssim k^{-\frac{\beta}{3}} W(s,k)^{-n}$$

holds for all $(s,k)\in[0,2P]\times[k_0,\infty)$.

4 Galerkin boundary element methods and convergence analyses

Throughout this section we assume that an integral equation formulation

$$\mathcal{R}_k\eta = f \tag{28}$$

is given to deal with the problem (4) where $\mathcal{R}_k : L^2(\partial K) \to L^2(\partial K)$ is continuous and coercive for all $k \geq k_0$ for some $k_0 > 1$, with continuity and coercivity constants C_k and c_k. We also assume that $\sigma_\beta^{\text{slow}}$ (12) is available for some $\beta \in \mathbb{Z}_+$. This amounts to assuming that the terms $a_{p,q,r,\ell}$ in the asymptotic expansion of η^{slow} appearing in the definition of $\sigma_\beta^{\text{slow}}$ are explicitly known throughout the entire boundary ∂K. This, in turn, means that a few of the terms in the asymptotic expansions of the "reflection" and the "diffraction" terms are explicitly known on the corresponding parts of the boundary. In this case, (28) can be re-written in terms of the new unknown $\rho_\beta = \eta - \sigma_\beta$ as

$$\mathcal{R}_k \rho_\beta = f_\beta \tag{29}$$

where $f_\beta = f - \mathcal{R}_k \sigma_\beta$. Note that $\rho_\beta = \eta$ and $f_\beta = f$ when $\beta = 0$.

Definition 3 We define the *β-asymptotic Galerkin approximation $\hat{\eta}_\beta$ to η* associated with a finite dimensional subspace $\mathcal{G}$ of $L^2(\partial K)$ as

$$\hat{\eta}_\beta := \sigma_\beta + \hat{\rho}_\beta \in \sigma_\beta + \mathcal{G} \tag{30}$$

where $\hat{\rho}_\beta \in \mathcal{G}$ is the unique solution to the Galerkin formulation

$$\langle \hat{\mu}, \mathcal{R}_k \hat{\rho}_\beta \rangle = \langle \hat{\mu}, f_\beta \rangle, \qquad \text{for all } \hat{\mu} \in \mathcal{G}, \tag{31}$$

of the integral equation (29).

In virtue of (30) and Definition 1, we observe that $\eta - \hat{\eta}_\beta = \rho_\beta - \hat{\rho}_\beta$. Accordingly, the Galerkin approximation spaces defined in the form

$$\mathcal{G} = e^{ik\,\alpha\cdot\gamma}\,\mathcal{G}^{\text{slow}}$$

capture the oscillations in $\rho_\beta = e^{ik\,\alpha\cdot\gamma}\,\rho_\beta^{\text{slow}}$ exactly. This, in turn, reduces the problem to the design of approximation spaces $\mathcal{G}^{\text{slow}}$ so as to effectively resolve the boundary layers of ρ_β^{slow}, as implied by Theorem 3, around the shadow boundaries with increasing k. In Sects. 4.1 and Sect. 4.2, we introduce two different Galerkin approximation spaces that are designed to effectively resolve the aforementioned boundary layers, and where their convergence analyses are also presented. In particular, these analyses reveal that the explicit knowledge of σ_β implies that, provided the stability constant C_k/c_k grows like k^ϱ as $k \to \infty$ for some $\varrho > 0$, then it can be controlled by $k^{-\beta/3}$ choosing $\beta > 3\varrho$.

The design of *frequency-adapted β-asymptotic Galerkin approximation space* in Sect. 4.1 and the *β-asymptotic Galerkin approximation space based on frequency dependent changes of variables* in Sect. 4.2, replicate those proposed for solution of the corresponding Dirichlet problem in [26] and [25] respectively. However, the convergence analyses have non-trivial technicalities due to the differences between the wavenumber dependent estimates on the derivatives of the densities (total field for the Neumann problem and normal derivative of total field for the Dirichlet problem).

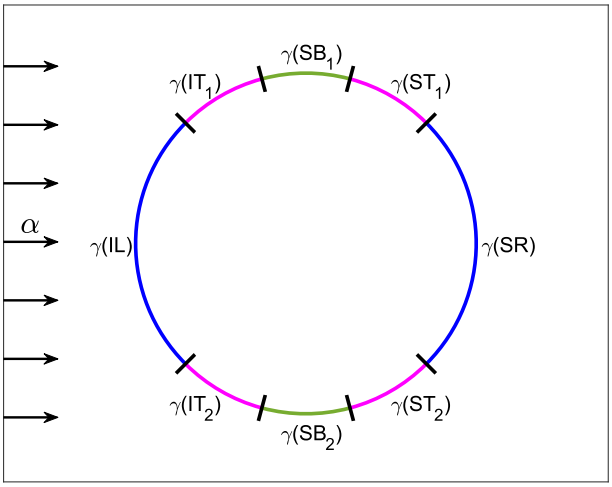

Fig. 3 Parameterized regions for a plane-wave with direction $\alpha = (1, 0)$ on a circle

For the sake of presentation, we refer to [25, 26] for additional details on the proofs if needed.

4.1 Frequency-adapted β-asymptotic Galerkin boundary element method

For the construction of β-asymptotic frequency-adapted Galerkin approximation spaces, given $k \geq 1$, a natural number m, real numbers $\epsilon_1, \ldots, \epsilon_m$ with $0 < \epsilon_m < \epsilon_{m-1} < \cdots < \epsilon_1 < \frac{1}{3}$, and positive real numbers $\xi_1, \xi_2, \zeta_1, \zeta_2$ satisfying $t_1 - \xi_1 < t_2 - \xi_2$ and $t_2 + \zeta_2 < 2P + t_1 - \zeta_1$, the *illuminated region* (IL), *illuminated transitions* (IT_1 and IT_2), *shadow transitions* (ST_1 and ST_2), *shadow boundaries* (SB_1 and SB_2), and *shadow region* (SR), in the parameter domain are defined as

$$
\begin{aligned}
IL &:= [t_1 + \xi_1 k^{-\frac{1}{3}+\epsilon_1}, t_2 - \xi_2 k^{-\frac{1}{3}+\epsilon_1}],\\
IT_1 &:= [t_1 + \xi_1 k^{-\frac{1}{3}+\epsilon_m}, t_1 + \xi_1 k^{-\frac{1}{3}+\epsilon_1}],\\
IT_2 &:= [t_2 - \xi_2 k^{-\frac{1}{3}+\epsilon_1}, t_2 - \xi_2 k^{-\frac{1}{3}+\epsilon_m}],\\
SB_1 &:= [t_1 - \zeta_1 k^{-\frac{1}{3}+\epsilon_m}, t_1 + \xi_1 k^{-\frac{1}{3}+\epsilon_m}],\\
SB_2 &:= [t_2 - \xi_1 k^{-\frac{1}{3}+\epsilon_m}, t_2 + \zeta_2 k^{-\frac{1}{3}+\epsilon_m}],\\
ST_1 &:= [t_1 - \zeta_1 k^{-\frac{1}{3}+\epsilon_1}, t_1 - \zeta_1 k^{-\frac{1}{3}+\epsilon_m}],\\
ST_2 &:= [t_2 + \zeta_2 k^{-\frac{1}{3}+\epsilon_m}, t_2 + \zeta_2 k^{-\frac{1}{3}+\epsilon_1}],\\
SR &:= [t_2 + \zeta_2 k^{-\frac{1}{3}+\epsilon_1}, 2P + t_1 - \zeta_1 k^{-\frac{1}{3}+\epsilon_1}];
\end{aligned}
$$

see Fig. 3 for sample illustrations of these regions.

Note that as $k \to \infty$ the illuminated and shadow regions cover the entire boundary in the parameter domain, and the remaining regions collapse to the shadow boundaries. In order to resolve the singularities of ρ_β^{slow} in vicinities of shadow boundaries as

implied by the wavenumber explicit derivative estimates in Theorem 3, for $m > 1$, we partition each one of the four transition regions into $m - 1$ subregions as

$$\begin{aligned} IT_1^j &:= [t_1 + \xi_1 k^{-\frac{1}{3}+\epsilon_{j+1}}, t_1 + \xi_1 k^{-\frac{1}{3}+\epsilon_j}], \\ IT_2^j &:= [t_2 - \xi_2 k^{-\frac{1}{3}+\epsilon_j}, t_2 - \xi_2 k^{-\frac{1}{3}+\epsilon_{j+1}}], \\ ST_1^j &:= [t_1 - \zeta_1 k^{-\frac{1}{3}+\epsilon_j}, t_1 - \zeta_1 k^{-\frac{1}{3}+\epsilon_{j+1}}], \\ ST_2^j &:= [t_2 + \zeta_2 k^{-\frac{1}{3}+\epsilon_{j+1}}, t_2 + \zeta_2 k^{-\frac{1}{3}+\epsilon_j}], \end{aligned}$$

for $j = 1, \ldots, m-1$. These result in a total of $4m$ regions

$$R_j := [a_j, b_j] := \begin{cases} IT_1^j, & j = 1, \ldots, m-1, \\ IT_2^{j-m}, & j = m+1, \ldots, 2m-1, \\ ST_1^{j-2m}, & j = 2m+1, \ldots, 3m-1, \\ ST_2^{j-3m}, & j = 3m+1, \ldots, 4m-1, \end{cases}$$

and

$$R_m := IL, \quad R_{2m} := SR, \quad R_{3m} := SB_1, \quad R_{4m} := SB_2,$$

with the transition regions being redundant when $m = 1$. Identifying the spaces $L^2(\partial K)$ and $L^2(\cup_{j=1}^{4m} R_j)$ through the parameterization γ, we now define the Galerkin approximation spaces, and the associated asymptotic Galerkin solutions.

Definition 4 For $m \in \mathbb{N}$ and $\mathbf{d} = (d_1, \ldots, d_{4m}) \in \mathbb{Z}_+^{4m}$, the $4m + |\mathbf{d}|$ dimensional *frequency-adapted Galerkin approximation space* in $L^2(\partial K)$ is defined as the direct sum

$$\mathcal{G}_{\mathbf{d}} := e^{ik\,\alpha\cdot\gamma}\, \mathcal{G}_{\mathbf{d}}^{\text{slow}} := e^{ik\,\alpha\cdot\gamma} \bigoplus_{j=1}^{4m} \mathbb{1}_{R_j}\, \mathbb{P}_{d_j} \tag{32}$$

where $\mathbb{1}_R$ is the characteristic function, and $\mathbb{P}_d$ is the space of polynomials of degree at most d.

Definition 5 For $m \in \mathbb{N}$ and $\mathbf{d} = (d_1, \ldots, d_{4m}) \in \mathbb{Z}_+^{4m}$, the *$\beta$-asymptotic frequency-adapted Galerkin approximation* $\hat{\eta}_\beta$ to η is defined as

$$\hat{\eta}_\beta := \sigma_\beta + \hat{\rho}_\beta \in \sigma_\beta + \mathcal{G}_{\mathbf{d}}$$

where σ_β is as given in (12), and $\hat{\rho}_\beta = e^{ik\,\alpha\cdot\gamma}\,\hat{\rho}_\beta^{\text{slow}} \in \mathcal{G}_{\mathbf{d}}$ is the unique solution of the Galerkin formulation

$$\langle \hat{\mu}, \mathcal{R}_k \hat{\rho}_\beta \rangle = \langle \hat{\mu}, f_\beta \rangle, \qquad \text{for all } \hat{\mu} \in \mathcal{G}_{\mathbf{d}},$$

of the integral equation (29).

The approximation properties of the β-asymptotic frequency-adapted Galerkin method are given in the following.

Theorem 4 *Given $m \in \mathbb{N}$ and $(n_1, \ldots, n_{4m}) \in \mathbb{Z}_+^{4m}$, for $k \geq k_0$ and all $\mathbf{d} = (d_1, \ldots, d_{4m}) \in \mathbb{N}^{4m}$ with $d_j \geq n_j - 1$, we have*

$$\|\eta - \hat{\eta}_\beta\|_{L^2(\partial K)} \lesssim \frac{C_k}{c_k} k^{-\frac{\beta}{3}} \sum_{j=1}^{4m} \frac{1 + E(k, j)}{(d_j)^{n_j}} \tag{33}$$

for the β-asymptotic frequency-adapted Galerkin approximation $\hat{\eta}_\beta \in \sigma_\beta + \mathcal{G}_{\mathbf{d}}$ to η. On the transition regions (with $j' = j \mod m$ and $j' \in \{1, \ldots, m-1\}$)

$$E(k, j) := k^{-\frac{1-3\epsilon_{j'}+1}{6}} (k^{\frac{\epsilon_{j'}-\epsilon_{j'+1}}{2}})^{n_j}, \qquad j \in \{1, \ldots, 4m\} \backslash \{m, 2m, 3m, 4m\},$$

on the illuminated and shadow regions

$$E(k, j) := \delta_{n_j,1} \sqrt{\log k} + H[n_j - 2] k^{-\frac{1-3\epsilon_1}{6}} (k^{\frac{1-3\epsilon_1}{6}})^{n_j}, \qquad j = m, 2m,$$

where δ and H are the Kronecker delta and Heaviside functions, and on the shadow boundaries

$$E(k, j) := k^{-\frac{1}{6}} \left(k^{\epsilon_m}\right)^{n_j}, \qquad j = 3m, 4m.$$

Proof Writing $\hat{\rho}_\beta = e^{ik\alpha\cdot\gamma} \hat{\rho}_\beta^{\text{slow}}$ for the unique solution of (31), we have

$$\eta - \hat{\eta}_\beta = (\sigma_\beta + \rho_\beta) - (\sigma_\beta + \hat{\rho}_\beta) = \rho_\beta - \hat{\rho}_\beta = e^{ik\alpha\cdot\gamma} \sum_{j=1}^{4m} \mathbb{1}_{R_j} (\rho_\beta^{\text{slow}} - \hat{\rho}_\beta^{\text{slow}}). \tag{34}$$

Accordingly, when $\mathcal{G} = \mathcal{G}_{\mathbf{d}}$, using Céa's lemma, we obtain

$$\begin{aligned}
\|\eta - \hat{\eta}_\beta\| &= \|\sum_{j=1}^{4m} \mathbb{1}_{R_j} (\rho_\beta^{\text{slow}} - \hat{\rho}_\beta^{\text{slow}})\| \\
&\leq \frac{C_k}{c_k} \inf\{\|\sum_{j=1}^{4m} \mathbb{1}_{R_j} (\rho_\beta^{\text{slow}} - p_j)\| : (p_1, \ldots, p_{4m}) \in \mathbb{P}_{d_1} \times \ldots \times \mathbb{P}_{d_{4m}}\} \\
&\leq \frac{C_k}{c_k} \sum_{j=1}^{4m} \inf_{p_j \in \mathbb{P}_{d_j}} \|\rho_\beta^{\text{slow}} - p_j\|_{L^2([a_j, b_j])}.
\end{aligned}$$

Therefore, by Theorem 3 above and Theorem 9 in Appendix 1, we have

$$\|\eta - \hat{\eta}_\beta\| \lesssim \frac{C_k}{c_k} k^{-\frac{\beta}{3}} \sum_{j=1}^{4m} \frac{\mathcal{W}(k; n_j; a_j, b_j)}{(d_j)^{n_j}}$$

for all positive integers $d_j \geq n_j - 1$ $(j = 1, \ldots, 4m)$ where

$$\mathcal{W}(k; n; a, b) := \left[\int_a^b \frac{(s-a)^n (b-s)^n}{W(s,k)^{2n}} \, ds \right]^{\frac{1}{2}}. \tag{35}$$

This inequality when combined with the next lemma gives the desired result. □

Lemma 4 *For all $n \in \mathbb{Z}_+$ and all $k \geq 1$, we have:*

(i) Illuminated and shadow regions: If $0 < \epsilon < \frac{1}{3}$, $a = t_1 + \xi_1 k^{-\frac{1}{3}+\epsilon}$ and $b = t_2 - \xi_2 k^{-\frac{1}{3}+\epsilon}$, or $a = t_2 + \zeta_2 k^{-\frac{1}{3}+\epsilon}$ and $b = 2P + t_1 - \zeta_1 k^{-\frac{1}{3}+\epsilon}$, then

$$\mathcal{W}(k; n; a, b) \lesssim 1 + \delta_{n,1} \sqrt{\log k} + H[n-2] k^{\frac{1-3\epsilon}{6}(n-1)}. \tag{36}$$

(ii) Illuminated and shadow transitions: If $0 < \delta < \epsilon < \frac{1}{3}$, $a = t_1 + \xi_1 k^{-\frac{1}{3}+\delta}$ and $b = t_1 + \xi_1 k^{-\frac{1}{3}+\epsilon}$, or $a = t_1 - \zeta_1 k^{-\frac{1}{3}+\epsilon}$ and $b = t_1 - \zeta_1 k^{-\frac{1}{3}+\delta}$, or $a = t_2 + \zeta_2 k^{-\frac{1}{3}+\delta}$ and $b = t_2 + \zeta_2 k^{-\frac{1}{3}+\epsilon}$, or $a = t_2 - \xi_2 k^{-\frac{1}{3}+\epsilon}$ and $b = t_2 - \xi_2 k^{-\frac{1}{3}+\delta}$, then

$$\mathcal{W}(k; n; a, b) \lesssim 1 + k^{-\frac{1-3\delta}{6}} k^{\frac{\epsilon-\delta}{2} n}. \tag{37}$$

(iii) Shadow boundaries: If $0 \leq \epsilon, \delta < \frac{1}{3}$, $a = t_1 - \zeta_1 k^{-\frac{1}{3}+\delta}$ and $b = t_1 + \xi_1 k^{-\frac{1}{3}+\epsilon}$, or $a = t_2 - \xi_1 k^{-\frac{1}{3}+\epsilon}$ and $b = t_2 + \zeta_2 k^{-\frac{1}{3}+\delta}$, then

$$\mathcal{W}(k; n; a, b) \lesssim 1 + k^{-\frac{1}{6}} k^{\frac{\epsilon+\delta}{2} n}. \tag{38}$$

Proof In each of the three cases, the analyses leading into the given estimates are similar for each of the given pairs of parameters a and b, so we present the proof for only the very first pairs.

In any case, we have

$$\mathcal{W}(k; 0; a, b) = (b-a)^{\frac{1}{2}} \lesssim 1, \tag{39}$$

so we assume $n \geq 1$. When $1 \leq k \leq k_0$ for some $k_0 > 1$, we clearly have

$$\mathcal{W}(k; n; a, b) \lesssim 1, \tag{40}$$

and therefore we can assume that k is sufficiently large. In this case, for $W(s,k)$ defined in (18), we have

$$W(s,k) = \begin{cases} (s - c_I)(d_I - s), & s \in [t_1, t_2], \\ (c_S - s)(d_S - s), & s \in [0, 2P] \backslash [t_1, t_2], \end{cases} \tag{41}$$

where

$$c_I := P - \sqrt{T^2 + k^{-\frac{1}{3}}}, \qquad d_I := P + \sqrt{T^2 + k^{-\frac{1}{3}}},$$

and

$$c_S := P - \sqrt{T^2 - k^{-\frac{1}{3}}}, \qquad d_S := P + \sqrt{T^2 - k^{-\frac{1}{3}}},$$

wherein $T := \frac{t_2 - t_1}{2}$.

For (i) and (ii), we use (41) in Lemma 9 in Appendix 1 to obtain

$$\mathcal{W}(k; n; a, b)^2 = \sum_{\substack{0 \le p,q \le n \\ 1 \le j \le 2n}} \binom{4n-j-1}{2n-j} \binom{n}{p} \binom{n}{q} \frac{(-1)^n \, \mathcal{F}(a, b; a, b; c_I, d_I; n, p, q; j)}{(d_I - c_I)^{4n-j}} \tag{42}$$

where for $2n - (p + q + j) = -1$

$$\mathcal{F}(a, b; a, b; c_I, d_I; n, p, q; j) = (c_I - a)^p \, (c_I - b)^q \log\left(\frac{b - c_I}{a - c_I}\right) + (a - d_I)^p \, (b - d_I)^q \log\left(\frac{d_I - a}{d_I - b}\right),$$

and for $2n - (p + q + j) \neq -1$

$$\begin{aligned} &\mathcal{F}(a, b; a, b; c_I, d_I; n, p, q; j) \\ &= \frac{(c_I - a)^p \, (c_I - b)^q}{2n - (p + q + j) + 1} \left[(b - c_I)^{2n-(p+q+j)+1} - (a - c_I)^{2n-(p+q+j)+1}\right] \\ &\quad + \frac{(a - d_I)^p \, (b - d_I)^q}{2n - (p + q + j) + 1} \left[(d_I - a)^{2n-(p+q+j)+1} - (d_I - b)^{2n-(p+q+j)+1}\right]. \end{aligned}$$

For (i), as $k \to \infty$, we have $a - c_I \asymp k^{-\frac{1}{3}+\epsilon}$, $b - c_I \asymp 1$, $d_I - a \asymp 1$, and $d_I - b \asymp k^{-\frac{1}{3}+\epsilon}$ (see Remark 1 for the notation $\asymp$). Accordingly, for $0 \le p, q \le n$ and $1 \le j \le 2n$, we get

$$\begin{aligned} |\mathcal{F}(a, b; a, b; c_I, d_I; n, p, q; j)| &\lesssim 1 + (k^{-\frac{1}{3}+\epsilon})^p \, \log k + (k^{-\frac{1}{3}+\epsilon})^q \, \log k \\ &\lesssim 1 + \log k \end{aligned}$$

for $2n - (p + q + j) = -1$, and

$$\begin{aligned} |\mathcal{F}(a, b; a, b; c_I, d_I; n, p, q; j)| &\lesssim 1 + (k^{-\frac{1}{3}+\epsilon})^{2n-(q+j)+1} + (k^{-\frac{1}{3}+\epsilon})^{2n-(p+j)+1} \\ &\lesssim 1 + (k^{\frac{1}{3}-\epsilon})^{n-1} \end{aligned}$$

for $2n-(p+q+j)\neq -1$. Using these estimates in (42), and upon noting that $d_I-c_I\asymp 1$ as $k\to\infty$, we obtain

$$\mathcal{W}(k;n;a,b)^2\lesssim 1+\delta_{n,1}\,\log k+H[n-2]\,(k^{\frac{1}{3}-\epsilon})^{n-1},$$

and therefore (36) follows.

For (ii), as $k\to\infty$, we have $a-c_I\asymp k^{-\frac{1}{3}+\delta}$, $b-c_I\asymp k^{-\frac{1}{3}+\epsilon}$, $d_I-a\asymp 1$, and $d_I-b\asymp 1$ so that, for $0\le p,q\le n$ and $1\le j\le 2n$, we get

$$|\mathcal{F}(a,b;a,b;c_I,d_I;n,p,q;j)|\ \lesssim 1+(k^{-\frac{1}{3}+\delta})^p(k^{-\frac{1}{3}+\epsilon})^q\log k\lesssim 1$$

when $2n-(p+q+j)=-1$, and

$$\begin{aligned}
&|\mathcal{F}(a,b;a,b;c_I,d_I;n,p,q;j)|\\
&\lesssim 1+(k^{-\frac{1}{3}+\delta})^p\,(k^{-\frac{1}{3}+\epsilon})^q[(k^{-\frac{1}{3}+\delta})^{2n-(p+q+j)+1}+(k^{-\frac{1}{3}+\epsilon})^{2n-(p+q+j)+1}]\\
&\lesssim 1+(k^{-\frac{1}{3}+\delta})^{2n-j+1}\,(k^{\epsilon-\delta})^q+(k^{-\frac{1}{3}+\epsilon})^{2n-j+1}\,(k^{\delta-\epsilon})^q\\
&\lesssim 1+k^{-\frac{1}{3}+\delta}\,(k^{\epsilon-\delta})^n+k^{-\frac{1}{3}+\epsilon}\\
&\lesssim 1+k^{-\frac{1}{3}+\delta}\,(k^{\epsilon-\delta})^n
\end{aligned}$$

when $2n-(p+q+j)\neq -1$. Using these two estimates in (42) and recalling $d_I-c_I\asymp 1$ as $k\to\infty$, we therefore obtain

$$\mathcal{W}(k;n;a,b)^2\lesssim 1+H[n-2]\,k^{-\frac{1}{3}+\delta}\,(k^{\epsilon-\delta})^n$$

from which (37) follows.

As for (iii), Lemma 9 in Appendix 1 entails

$$\begin{aligned}
\mathcal{W}(k;n;a,b)^2=&\sum_{\substack{0\le p,q\le n\\ 1\le j\le 2n}}\binom{4n-j-1}{2n-j}\binom{n}{p}\binom{n}{q}(-1)^n\\
&\times\left\{\frac{\mathcal{F}(a,t_1;a,b;c_S,d_S;n,p,q;j)}{(d_S-c_S)^{4n-j}}+\frac{\mathcal{F}(t_1,b;a,b;c_I,d_I;n,p,q;j)}{(d_I-c_I)^{4n-j}}\right\},
\end{aligned}\tag{43}$$

and we need to estimate $\mathcal{F}(a,t_1;a,b;c_S,d_S;n,p,q,j)$ along with the term $\mathcal{F}(t_1,b;a,b;c_I,d_I;n,p,q;j)$. Considering the former, we have

$$\begin{aligned}
\mathcal{F}(a,t_1;a,b;c_S,d_S;n,p,q,j)=&(c_S-a)^p(c_S-b)^q\log\Big(\frac{t_1-c_S}{a-c_S}\Big)\\
&+(a-d_S)^p(b-d_S)^q\log\Big(\frac{d_S-a}{d_S-t_1}\Big)
\end{aligned}$$

for $2n-(p+q+j)=-1$, and

$$\begin{aligned}&\mathcal{F}(a,t_1;a,b;c_S,d_S;n,p,q,j)\\&\quad=\frac{(c_S-a)^p(c_S-b)^q}{2n-(p+q+j)+1}\left[(t_1-c_S)^{2n-(p+q+j)+1}-(a-c_S)^{2n-(p+q+j)+1}\right]\\&\qquad+\frac{(a-d_S)^p(b-d_S)^q}{2n-(p+q+j)+1}\left[(d_S-a)^{2n-(p+q+j)+1}-(d_S-t_1)^{2n-(p+q+j)+1}\right]\end{aligned}$$

for $2n-(p+q+j)\neq -1$. Since $c_S-a\asymp k^{-\frac{1}{3}+\delta}$, $|c_S-b|\lesssim k^{-\frac{1}{3}+\epsilon}$, $c_S-t_1\asymp k^{-\frac{1}{3}}$, $d_S-a\asymp 1$, $d_S-b\asymp 1$, $d_S-t_1\asymp 1$, and $d_S-c_S\asymp 1$ so that, for $0\leq p,q\leq n$ and $1\leq j\leq 2n$, we get

$$\mathcal{F}(a,t_1;a,b;c_S,d_S;n,p,q,j)\lesssim 1+(k^{-\frac{1}{3}+\delta})^p(k^{-\frac{1}{3}+\epsilon})^q\log k\lesssim 1$$

for $2n-(p+q+j)=-1$, and

$$\begin{aligned}&\mathcal{F}(a,t_1;a,b;c_S,d_S;n,p,q,j)\\&\quad\lesssim 1+(k^{-\frac{1}{3}+\delta})^p(k^{-\frac{1}{3}+\epsilon})^q\left[(k^{-\frac{1}{3}})^{2n-(p+q+j)+1}+(k^{-\frac{1}{3}+\delta})^{2n-(p+q+j)+1}\right]\\&\quad\lesssim 1+(k^{-\frac{1}{3}})^{2n-j+1}(k^{\delta})^p(k^{\epsilon})^q+(k^{-\frac{1}{3}+\delta})^{2n-j+1}(k^{\epsilon-\delta})^q\\&\quad\lesssim 1+k^{-\frac{1}{3}}\,(k^{\epsilon+\delta})^n+k^{-\frac{1}{3}+\delta}\,(k^{\epsilon-\delta})^n\\&\quad\lesssim 1+k^{-\frac{1}{3}}\,(k^{\epsilon+\delta})^n\end{aligned}$$

for $2n-(p+q+j)\neq -1$. The same estimates hold also for the relevant term $\mathcal{F}(t_1,b;a,b;c_I,d_I;n,p,q;j)$. Accordingly (43) implies

$$\mathcal{W}(k;n;a,b)^2\lesssim 1+k^{-\frac{1}{3}}\,(k^{\epsilon+\delta})^n,$$

and this yields (38). □

In Theorem 4, for a given $n\in\mathbb{Z}_+$, taking $n_1=\ldots=n_{4m}=n$ and setting $d_1=\ldots=d_{4m}=d$ for any positive integer $d\geq n-1$, we see that in order to balance the errors in all the $4m$ regions uniformly for all n (cf. (33)), we must have

$$\frac{1-3\epsilon_1}{6}=\epsilon_m=\frac{\epsilon_j-\epsilon_{j+1}}{2},\qquad j=1,\ldots,m-1.$$

This system of equations can be explicitly solved to yield the following.

Corollary 2 *Given $n\in\mathbb{Z}_+$ and $m\in\mathbb{N}$, if ϵ_j are chosen as*

$$\epsilon_j:=\frac{1}{3}\,\frac{2m-2j+1}{2m+1},\qquad j=1,\ldots,m,\tag{44}$$

then, for all $k \geq k_0$ *and* $\mathbf{d} := (d, \ldots, d) \in \mathbb{N}^{4m}$ *with* $d \geq n-1$, *we have*

$$\|\eta - \hat{\eta}_\beta\|_{L^2(\partial K)} \lesssim \frac{C_k}{c_k} k^{-\frac{\beta}{3}} m \frac{1 + \delta_{n,1}\sqrt{\log k} + H[n-2]\,(k^{\frac{1}{6m+3}})^{n-1}}{d^n} \tag{45}$$

for the β*-asymptotic frequency-adapted Galerkin approximation* $\hat{\eta}_\beta \in \sigma_\beta + \mathcal{G}_{\mathbf{d}}$ *to* η.

To our knowledge, explicit analytical representations of the terms $a_{p,q,r,\ell}$ in the ansatz (9) are not available and this corresponds to $\beta = 0$. However, when the number of subregions m is chosen to increase proportional to $\log(k^{\frac{1}{6}})$ (which is clearly proportional to $\log(k)$), we observe that $k^{\frac{1}{6m+3}}$ is bounded and therefore (45) implies

$$\|\eta - \hat{\eta}_\beta\|_{L^2(\partial K)} \lesssim \frac{C_k}{c_k} \log(k) \frac{1 + \delta_{n,1}\sqrt{\log(k)}}{d^n}. \tag{46}$$

Moreover, as $k \to \infty$, if the stability constant $\frac{C_k}{c_k}$ grows proportional to k^{ϱ_1} for some $\varrho_1 > 0$, and d is chosen to grow as k^{ϱ_2} for some $\varrho_2 > 0$, then

$$\frac{C_k}{c_k} \log(k) \frac{1 + \delta_{n,1}\sqrt{\log(k)}}{d^n} \lesssim k^{\varrho_1} \frac{(\log(k))^{\frac{3}{2}}}{k^{n\varrho_2}} \lesssim 1$$

for all sufficiently large n. Since (46) is valid for all n, we therefore deduce that the convergence of the method is spectral and requires an increase of only $\mathcal{O}(k^\epsilon)$ (for any $\epsilon > 0$) in the total number of degrees of freedom to maintain accuracy for higher values of k.

One of the most important aspects of this method consists of incorporating sufficiently many terms $a_{p,q,r,\ell}$ in the ansatz (9) into the integral equation in order to obtain a frequency independent method. Indeed, when $\beta \in \mathbb{Z}_+$ is chosen so that $\frac{C_k}{c_k} k^{-\frac{\beta}{3}} (\log k)^{\frac{3}{2}} \lesssim 1$ as $k \to \infty$, then

$$\|\eta - \hat{\eta}_\beta\|_{L^2(\partial K)} \lesssim \frac{1}{d^n}.$$

This shows that the method is not only spectral but also independent of frequency in the sense that prescribed accuracies can be attained with the utilization of fixed numbers of degrees of freedom.

4.2 β-asymptotic Galerkin boundary element method based on frequency dependent changes of variables

For the construction of β-asymptotic Galerkin approximation spaces based on frequency dependent changes of variables, given positive constants $\xi_j, \xi_j', \zeta_j, \zeta_j'$, $j = 1, 2$, satisfying

$$t_1 + \xi_1 \leq t_1 + \xi_1' = t_2 - \xi_2' \leq t_2 - \xi_2,$$

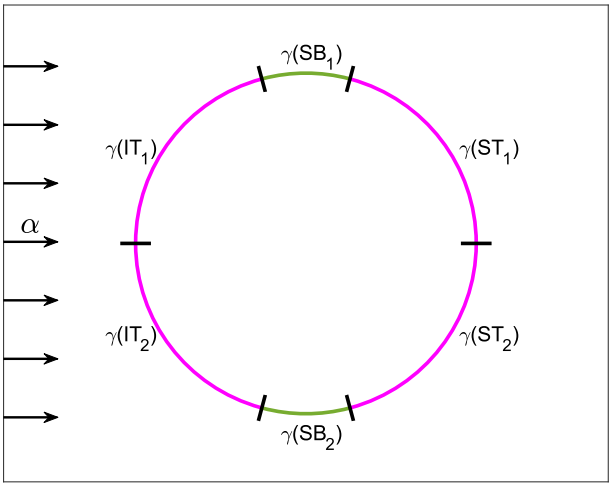

Fig. 4 Parametrized regions for a plane-wave with direction $\alpha = (1, 0)$ on a circle

$$t_2 + \zeta_2 \leq t_2 + \zeta_2' = 2P + t_1 - \zeta_1' \leq 2P + t_1 - \zeta_1,$$

we define, for any wavenumber $k > 1$, the *illuminated transition regions* as

$$\mathcal{I}_1 := [a_1, b_1] := [t_1 + \xi_1 k^{-\frac{1}{3}}, t_1 + \xi_1'], \quad \mathcal{I}_2 := [a_2, b_2] := [t_2 - \xi_2', t_2 - \xi_2 k^{-\frac{1}{3}}],$$

shadow transition regions as

$$\mathcal{I}_3 := [a_3, b_3] := [t_1 - \zeta_1', t_1 - \zeta_1 k^{-\frac{1}{3}}], \quad \mathcal{I}_4 := [a_4, b_4] := [t_2 + \zeta_2 k^{-\frac{1}{3}}, t_2 + \zeta_2'],$$

and the *shadow boundary regions* as

$$\begin{aligned} \mathcal{I}_5 &:= [a_5, b_5] := [t_1 - \zeta_1 k^{-\frac{1}{3}}, t_1 + \xi_1 k^{-\frac{1}{3}}], \\ \mathcal{I}_6 &:= [a_6, b_6] := [t_2 - \xi_2 k^{-\frac{1}{3}}, t_2 + \zeta_2 k^{-\frac{1}{3}}]; \end{aligned}$$

see Fig. 4 for a sample illustration of these regions.

In what follows we identifty $L^2(\partial K)$ and $L^2(\cup_{j=1}^6 \mathcal{I}_j)$ through the parametrization γ.

In order to capture the boundary layers of ρ_β in the transition regions as implied by Theorem 3, we introduce the frequency dependent changes of variables $\phi_j : \mathcal{I}_j \to \mathcal{I}_j$ by setting

$$\begin{aligned} \phi_1(s) &:= t_1 + \varphi_1(s)\, k^{\psi_1(s)}, & \phi_2(s) &:= t_2 - \varphi_2(s)\, k^{\psi_2(s)}, \\ \phi_3(s) &:= t_1 - \varphi_3(s)\, k^{\psi_3(s)}, & \phi_4(s) &:= t_2 + \varphi_4(s)\, k^{\psi_4(s)}, \\ \phi_5(s) &:= s, & \phi_6(s) &:= s. \end{aligned}$$

Here ψ_j are constructed so as to linearly increase from $-\frac{1}{3}$ to 0 as one moves away from the shadow boundaries, and φ_j are linear functions chosen to ensure that the maps $\phi_j : \mathcal{I}_j \to \mathcal{I}_j$ are bijective. They are defined explicitly as

$$\begin{aligned}
\psi_1(s) &:= -\frac{1}{3}\frac{b_1 - s}{b_1 - a_1}, \qquad & \varphi_1(s) &:= \xi_1 + \left(\xi_1' - \xi_1\right)\frac{s - a_1}{b_1 - a_1},\\
\psi_2(s) &:= -\frac{1}{3}\frac{s - a_2}{b_2 - a_2}, \qquad & \varphi_2(s) &:= \xi_2' + \left(\xi_2 - \xi_2'\right)\frac{s - a_2}{b_2 - a_2},\\
\psi_3(s) &:= -\frac{1}{3}\frac{s - a_3}{b_3 - a_3}, \qquad & \varphi_3(s) &:= \zeta_1' + \left(\zeta_1 - \zeta_1'\right)\frac{s - a_3}{b_3 - a_3},\\
\psi_4(s) &:= -\frac{1}{3}\frac{b_4 - s}{b_4 - a_4}, \qquad & \varphi_4(s) &:= \zeta_2 + \left(\zeta_2' - \zeta_2\right)\frac{s - a_4}{b_4 - a_4}.
\end{aligned}$$

With these definitions, we are now ready to introduce the Galerkin approximation spaces and the associated asymptotic solutions.

Definition 6 For $\mathbf{d} = (d_1, \ldots, d_6) \in \mathbb{Z}_+^6$, the *Galerkin approximation space based on frequency dependent changes of variables* of dimension $6 + |\mathbf{d}|$ in $L^2(\partial K)$ is defined as

$$\mathcal{C}_{\mathbf{d}} := e^{ik\,\alpha\cdot\gamma}\,\mathcal{C}_{\mathbf{d}}^{\text{slow}} := e^{ik\,\alpha\cdot\gamma}\bigoplus_{j=1}^{6} \mathbb{1}_{\mathcal{I}_j}\,\mathbb{P}_{d_j}\circ\phi_j^{-1}. \tag{47}$$

Definition 7 Given $\beta \in \mathbb{Z}_+$, the *β-asymptotic Galerkin approximation $\hat{\eta}_\beta$ to η based on frequency dependent changes of variables* is defined as

$$\hat{\eta}_\beta := \sigma_\beta + \hat{\rho}_\beta \in \sigma_\beta + \mathcal{C}_{\mathbf{d}} \tag{48}$$

where $\hat{\rho}_\beta := e^{ik\,\alpha\cdot\gamma}\hat{\rho}_\beta^{\text{slow}} \in \mathcal{C}_{\mathbf{d}}$ is the unique solution to the Galerkin formulation

$$\langle \hat{\mu}, \mathcal{R}_k\hat{\rho}_\beta\rangle = \langle \hat{\mu}, f_\beta\rangle, \qquad \text{for all } \hat{\mu} \in \mathcal{C}_{\mathbf{d}},$$

of the integral equation (29).

The convergence properties of the β-asymptotic Galerkin approximations $\hat{\eta}_\beta$ to η based on frequency dependent changes of variables are as summarized in the next theorem.

Theorem 5 *Given $(n_1, \ldots, n_6) \in \mathbb{Z}_+^6$, for all $k \geq k_0$ and $\mathbf{d} := (d_1, \ldots, d_6) \in \mathbb{N}^6$ with $d_j \geq n_j - 1$, we have*

$$\|\eta - \hat{\eta}_\beta\| \lesssim \frac{C_k}{c_k}k^{-\frac{\beta}{3}}\sqrt{\log k}\left(\sum_{j=1}^{4}(\log k)^{n_j}(d_j)^{-n_j} + \sum_{j=5}^{6}(d_j)^{-n_j}\right)$$

for the β-asymptotic Galerkin approximation $\hat{\eta}_\beta \in \sigma_\beta + \mathcal{C}_{\mathbf{d}}$ to η based on frequency dependent changes of variables.

Proof Arguing as in the proof of Theorem 4 and then changing variables, we obtain

$$\begin{aligned}\|\eta - \hat{\eta}_\beta\| &\leq \frac{C_k}{c_k} \sum_{j=1}^{6} \inf_{p_j \in \mathbb{P}_{d_j}} \|\rho_\beta^{\text{slow}} - p_j \circ \phi_j^{-1}\|_{L^2(\mathcal{I}_j)} \\ &= \frac{C_k}{c_k} \sum_{j=1}^{6} \inf_{p_j \in \mathbb{P}_{d_j}} \|(\rho_\beta^{\text{slow}} \circ \phi_j - p_j)\sqrt{\phi_j'}\|_{L^2(\mathcal{I}_j)}.\end{aligned}$$

Next we observe that $0 < \phi_j' \lesssim \log k$ on $\mathcal{I}_j$ for $j = 1, 2, 3, 4$. For instance, for $j = 1$, upon noting that $b_1 - a_1 \asymp 1$ (cf. Remark 1), $\psi_1 \leq 0$ on $\mathcal{I}_1$, and $0 < \xi_1 \leq \xi_1'$, this follows from the identity

$$\phi_1'(s) = \frac{1}{b_1 - a_1}\left[\xi_1' - \xi_1 + \frac{1}{3}\left(\xi_1 + (\xi_1' - \xi_1)\,\frac{s - a_1}{b_1 - a_1}\right)\log k\right] k^{\psi_1(s)}.$$

Further, we clearly have $\phi_j' = 1$ on $\mathcal{I}_j$ for $j = 4, 5$. Accordingly,

$$\|\eta - \hat{\eta}_\beta\| \lesssim \frac{C_k}{c_k}\sqrt{\log k} \sum_{j=1}^{6} \inf_{p_j \in \mathbb{P}_{d_j}} \|\rho_\beta^{\text{slow}} \circ \phi_j - p_j\|_{L^2(\mathcal{I}_j)}.$$

Theorem 9 in Appendix 1 therefore gives

$$\|\eta - \hat{\eta}_\beta\| \lesssim \frac{C_k}{c_k}\sqrt{\log k} \sum_{j=1}^{6} \frac{\left[\int_{a_j}^{b_j} |D_s^{n_j}(\rho_\beta^{\text{slow}} \circ \phi_j)(s)|^2 (s - a_j)^{n_j}(b_j - s)^{n_j} ds\right]^{\frac{1}{2}}}{(d_j)^{n_j}}.$$

Accordingly, since $b_j - a_j \asymp 1$ (cf. Remark 1) for $j = 1, 2, 3, 4$, and ϕ_5 and ϕ_6 are identity maps, the next lemma yields

$$\|\eta - \hat{\eta}_\beta\| \lesssim \frac{C_k}{c_k} k^{-\frac{\beta}{3}}\sqrt{\log k}\left(\sum_{j=1}^{4} \frac{(\log k)^{n_j}}{(d_j)^{n_j}} + \sum_{j=5}^{6} \frac{\mathcal{W}(k; n_j; a_j, b_j)}{(d_j)^{n_j}}\right)$$

where $\mathcal{W}$ is as defined in (35). Thus the result follows from part (iii) of Lemma 4. □

Lemma 5 *Given $k \geq k_0$ and $n \in \mathbb{N}$, the estimates*

$$|D_s^n(\rho_\beta^{\text{slow}} \circ \phi_j)| \lesssim k^{-\frac{\beta}{3}} \begin{cases} (\log k)^n, & j = 1, 2, 3, 4, \\ W(\cdot, k)^{-n}, & j = 5, 6, \end{cases} \tag{49}$$

hold on $\mathcal{I}_j$.

Proof For $n = 0$, the result is immediate from Theorem 3, so we assume $n \geq 1$. For $j = 1, \ldots, 4$, we utilize Faá Di Bruno's formula for the derivatives of a composition [39] to estimate

$$|D_s^n(\rho_\beta^{\text{slow}} \circ \phi_j)| \lesssim \sum_{(m_1,\ldots,m_n)\in\mathcal{F}_n} |(D_s^m \rho_\beta^{\text{slow}})(\phi_j)| \prod_{\ell=1}^{n} |D_s^\ell \phi_j|^{m_\ell}$$

where $\mathcal{F}_n = \{(m_1, \ldots, m_n) \in \mathbb{Z}_+^n : n = \sum_{\ell=1}^n \ell m_\ell\}$ and $m = \sum_{\ell=1}^n m_\ell$. Since [25,Proposition 4.3]

$$|D_s^\ell \phi_j| \lesssim (\log k)^\ell k^{\psi_j},$$

we therefore obtain

$$\begin{aligned} |D_s^n(\rho_\beta^{\text{slow}} \circ \phi_j)| &\lesssim (\log k)^n \sum_{(m_1,\ldots,m_n)\in\mathcal{F}_n} |(D_s^m \rho_\beta^{\text{slow}})(\phi_j)| k^{m\psi_j} \\ &\lesssim (\log k)^n \sum_{m=0}^{n} |(D_s^m \rho_\beta^{\text{slow}})(\phi_j)| k^{m\psi_j} \\ &\lesssim k^{-\frac{\beta}{3}} (\log k)^n \sum_{m=0}^{n} W(\phi_j, k)^{-m} k^{m\psi_j}, \end{aligned} \tag{50}$$

where the last inequality is a consequence of Theorem 3. Note that, since

$$W(\phi_j, k) = k^{-\frac{1}{3}} + |\omega(\phi_j)| > |\omega(\phi_j)| = |(\phi_j - t_1)(t_2 - \phi_j)|$$

and

$$\begin{aligned} \phi_1 - t_1 = \varphi_1 k^{\psi_1} \geq \varphi_1(a_1) k^{\psi_1} = \xi_1 k^{\psi_1}, \quad t_2 - \phi_1 \geq t_2 - \phi_1(b_1) = \xi_2' \quad &\text{on } \mathcal{I}_1, \\ \phi_2 - t_1 \geq \phi_2(a_2) - t_1 = \xi_1', \quad t_2 - \phi_2 = \varphi_2 k^{\psi_2} \geq \varphi_2(a_2) k^{\psi_2} = \xi_2' k^{\psi_2} \quad &\text{on } \mathcal{I}_2, \\ t_1 - \phi_3 = \varphi_3 k^{\psi_3} \geq \varphi_3(b_3) k^{\psi_3} = \zeta_1 k^{\psi_3}, \quad t_2 - \phi_3 > t_2 - t_1 \quad &\text{on } \mathcal{I}_3, \\ \phi_4 - t_1 > t_2 - t_1, \quad \phi_4 - t_2 = \varphi_4 k^{\psi_4} \geq \varphi_4(a_4) k^{\psi_4} = \zeta_2' k^{\psi_4} \quad &\text{on } \mathcal{I}_4, \end{aligned}$$

setting $\xi = \min\{\xi_1\xi_1', \xi_1'\xi_2', \zeta_1(t_2 - t_1), \zeta_2'(t_2 - t_1)\}$, we have

$$W(\phi_j, k)^{-1} k^{\psi_j} \leq \frac{1}{\xi^2} \quad \text{on } \mathcal{I}_j \tag{51}$$

for $j = 1, 2, 3, 4$. Use of (51) in (50) therefore proves (49) for $j = 1, 2, 3, 4$. Note that (49) is immediate from Theorem 3 for $j = 5, 6$ since, in this case, ϕ_j is the identity map on $\mathcal{I}_j$. This finishes the proof. □

Assigning the same local polynomial degree d to each interval $\mathcal{I}_j$, we obtain the following.

Corollary 3 *Given $n \in \mathbb{Z}_+$, for all $k \geq k_0$ and $\mathbf{d} := (d, \ldots, d) \in \mathbb{N}^6$ with $d \geq n-1$, we have*

$$\|\eta - \hat{\eta}_\beta\|_{L^2(\partial K)} \lesssim \frac{C_k}{c_k} k^{-\frac{\beta}{3}} \frac{(\log k)^{n+\frac{1}{2}}}{d^n} \tag{52}$$

for the β-asymptotic Galerkin approximation $\hat{\eta}_\beta \in \sigma_\beta + \mathcal{C}_{\mathbf{d}}$ to η based on frequency dependent changes of variables.

In the case that the stability constant C_k/c_k grows algebraically (that is $C_k/c_k \asymp k^\delta$ for some $\delta > 0$) as $k \to \infty$, Corollary 3 implies the followings. First, recall that $\beta = 0$ means no term $a_{p,q,r,\ell}$ in the ansatz (9) is incorporated into the integral equation (28). Still, even in this case, estimate (52) clearly implies that the method is not only spectral for each fixed k, but also increasing the number of degrees of freedom proportional to k^ϵ (for any $\epsilon > 0$) is sufficient to fix the approximation error with increasing k. In other words, the method is spectral and *almost* frequency independent. When $\beta > 0$ is chosen so that $\delta - \beta/3 < 0$, the method is still spectral for each fixed k, and moreover it is frequency independent in the sense that prescribed accuracies can be attained with the utilization of frequency independent numbers of degrees of freedom with increasing k.

5 Numerical results

In this section, we present numerical results validating the theoretical developments on the *β-asymptotic Galerkin boundary element method based on frequency dependent changes of variables* (GBemCV) described in Sect. 4.2. Since the explicit forms of the terms $a_{p,q,r,\ell}$ in the asymptotic expansion (9) are not available over the entire boundary ∂K, we take $\beta = 0$. The numerical results obtained using the *frequency-adapted β-asymptotic Galerkin boundary element method* detailed in Sect. 4.1 are entirely similar, and therefore not presented.

Several integral equations can be used to solve the Neumann problem (4), and they are expressed in the general form

$$\mathcal{R}_k \eta = f_k \quad \text{on } \partial K \tag{53}$$

where η is the total field [21]. Using standard techniques, the operator $\mathcal{R}_k$ and the right hand side f_k can be taken as

$$\begin{aligned} &\mathcal{R}_k := \mathcal{I} - 2\mathcal{K}_k, \qquad f_k := 2u^{\text{inc}} \\ &\mathcal{R}_k := \mathcal{T}_k, \qquad f_k := \partial_\nu u^{\text{inc}} \\ &\mathcal{R}_k := \mathcal{I} - 2(\mathcal{K}_k + i\mu\mathcal{T}_k), \qquad f_k := 2(u^{\text{inc}} - i\mu\partial_\nu u^{\text{inc}}) \end{aligned} \tag{54}$$

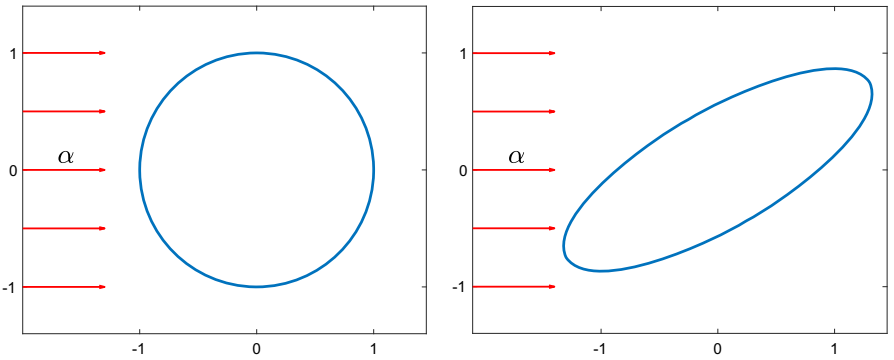

Fig. 5 Configurations used in the numerical tests

where μ is a real coupling parameter, and the double layer and hyper-singular operators are given respectively by

$$\mathcal{K}_k\phi(x) := \int_{\partial K} \frac{\partial G_k(x,y)}{\partial \nu(y)}\,\phi(y)\,ds(y),$$

and

$$\mathcal{T}_k\phi(x) := \frac{\partial}{\partial \nu(x)} \int_{\partial K} \frac{\partial G_k(x,y)}{\partial \nu(y)}\,\phi(y)\,ds(y).$$

For the numerical tests performed here, we choose to implement the integral equation (53) using (54) owing to the fact that it contains only integral operators with weakly singular kernels. We discretize the operator $\mathcal{R}_k$ through use of the trapezoidal rule and the Nyström method [20] utilizing 10 to 12 points per wavelength. Regarding the implementation, we refer to [25, 26] since it is similar to its Dirichlet version.

We consider two different single-scattering configurations consisting of the unit circle $\{(\cos t, \sin t) : t \in [0, 2\pi]\}$, and the ellipse $\{(\frac{3}{2}\cos t, \frac{1}{2}\sin t) : t \in [0, 2\pi]\}$ rotated by $\frac{\pi}{6}$ radians in the counterclockwise direction. In both cases, the illumination is coming in from the left as depicted in Fig. 5.

The unit circle is the standard test case since the analytical solution can be derived with the aid of Fourier analysis and Jacobi-Anger expansion [20]. For a circle of radius r, switching to polar coordinates, the analytical solution for the Neumann boundary value problem is expressed as

$$\eta(\theta) = e^{ikr\cos\theta} + \sum_{m\in\mathbb{Z}} i^{m+2} \frac{(J_m(kr))'}{(H_m^{(1)}(kr))'}\, e^{im\theta}\, H_m^{(1)}(kr) \tag{55}$$

where J_m and $H_m^{(1)}$ are, respectively, the Bessel and Hankel functions of the first kind and order m [1]. We display in Figure 6 the real and imaginary parts of the analytical solution η along with those of the envelope η^{slow} for $k = 50, 100, 200, 400, 800$.

We observe that the oscillations in the solution η are increasing with increasing frequency. In addition, as the asymptotic theory predicts, η^{slow} is non-oscillatory in the illuminated region, admits boundary layers around the shadow boundaries, and decays exponentially with increasing frequency in the deep shadow region. In order to validate the accuracy of the approximations, we compare in Fig. 7 the exact value and the numerical approximation of η for $k = 400$. We can see that the GBemCV solution successfully approximates the exact solution over the entire boundary.

We analyze now the error produced by the use of the GBemCV method. The strategy resides in evaluating the error with respect to increasing values of the local polynomial degree d (see Corollary 3). In Fig. 9 (left), we plot the logarithmic L^2-errors

$$\log_{10}(\|\eta - \hat{\eta}_\beta\|_{L^2}) \tag{56}$$

for $d = 4, 8, 12, 16, 20$ and $k = 50, 100, 200, 400, 800$. Let us mention that $\hat{\eta}_\beta$ is defined in (48), and η represents the analytical solution in (55). In our numerical tests, we have constructed the Galerkin approximation spaces $\mathcal{C}_{\mathbf{d}}$ in (47) utilizing the same local polynomial degree d on each of the six direct summands which generates the total number of degrees of freedom $6(d + 1)$. The results in Fig. 9 (left) show that, for any fixed value of k, the accuracy increases with increasing values of d, and the method is frequency independent.

For the elliptical configuration displayed in Fig. 5, since the analytical solution is not available, we first start by displaying in Fig. 8 the numerical solutions obtained by the GBemCV method (for $\beta = 0$). We can observe that η and η^{slow} exhibit properties similar to the circle case. More precisely, with increasing wavenumber, η^{slow} is non-oscillatory in the illuminated region, admits boundary layers around the shadow boundaries, and it decays exponentially in the deep shadow region. Concerning the error analysis, we plot in Fig. 9 (right) the local polynomial degree d versus logarithmic L^2-errors for $d = 4, 8, 12, 16, 20$ and $k = 50, 100, 200, 400, 800$. As mentioned above, in (56), $\hat{\eta}_\beta$ is defined in (48), however, η is computed using the Nyström method [20]. As in the case of the circle, the results in Fig. 9 (right) show that for any wavenumber the accuracy increases with the increasing local polynomial degree d, and the method is also frequency independent.

6 Conclusion

In this paper, we proposed two different β-asymptotic Galerkin boundary element methods for approximations of solutions to high-frequency sound-hard scattering problems. These two methods are based on the ansatz describing the asymptotic behavior of the total field associated with the Neumann boundary condition. We provided the missing parts in the derivation of this ansatz given in [45]. For the convergence analyses, we used the ansatz to derive wavenumber explicit estimates on the derivatives of the slow envelope corresponding to the total field on the boundary. An important ingredient of these analyses resides in the use of appropriate number of terms in the asymptotic expansion. This resulted in the design of Galerkin boundary element methods that deliver prescribed error tolerances using frequency independent numbers of

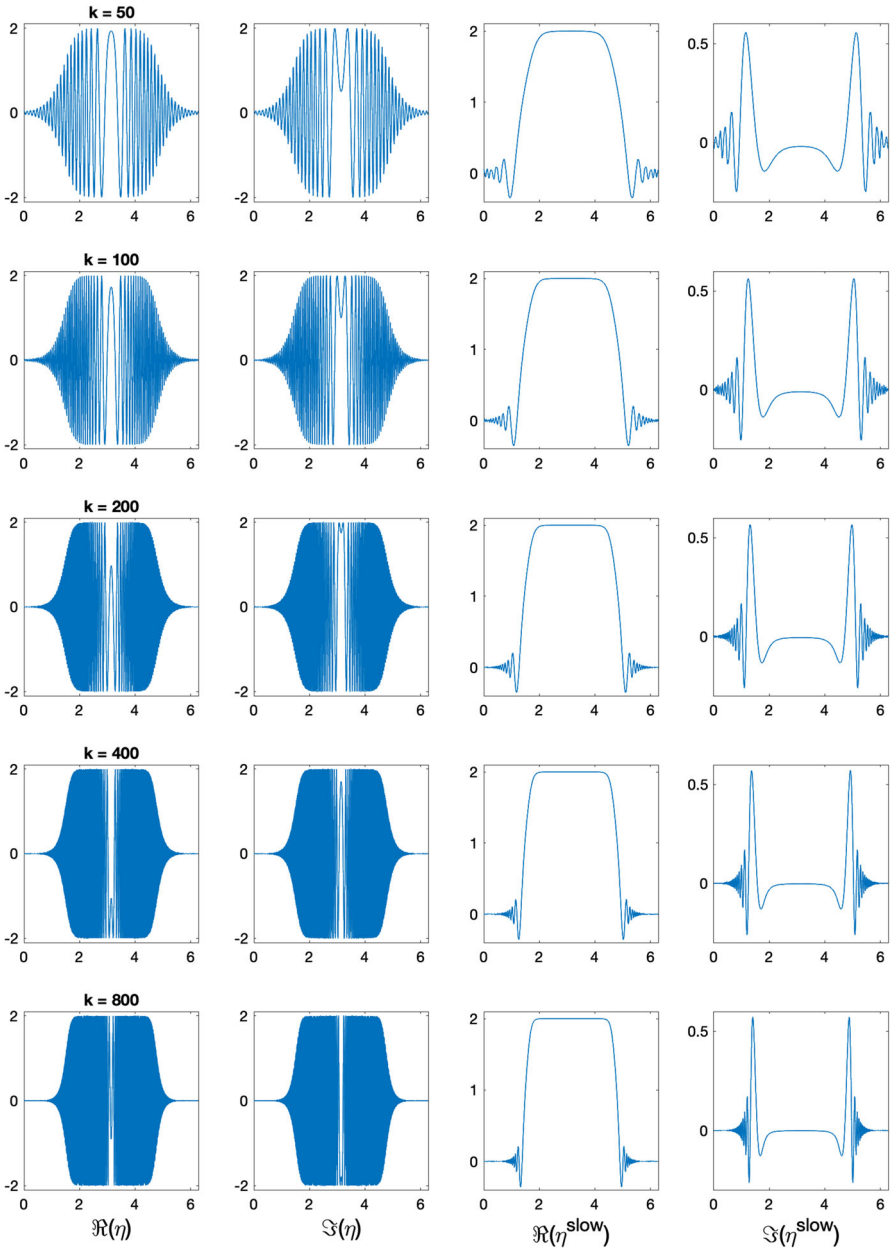

Fig. 6 Real (first column) and imaginary (second column) parts of η, and those of η^{slow} (columns three and four) associated with the circular scatterer in Fig. 5 for $k = 50, 100, 200, 400, 800$

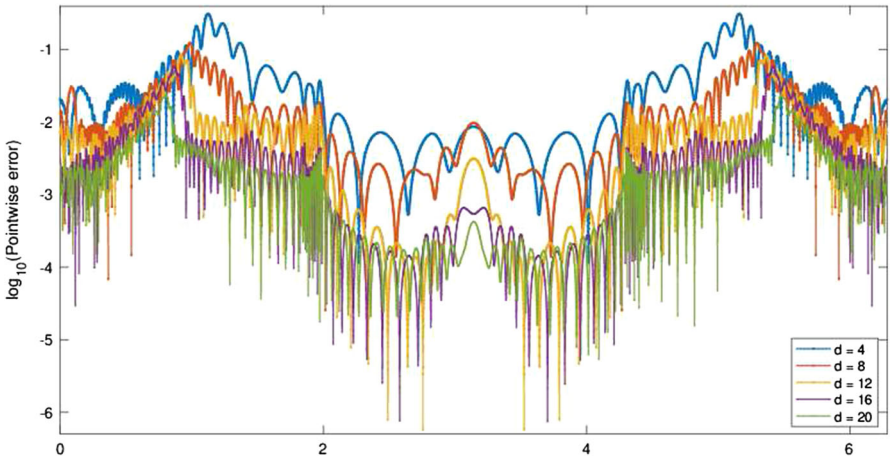

Fig. 7 Logarithmic pointwise errors for the unit circle in Fig. 5 for $k = 400$ and local polynomial degrees $d = 4, 8, 12, 16, 20$

degrees of freedom. The numerical implementations confirm that the solutions corresponding to any fixed number of degrees of freedom yield frequency independent approximations.

Acknowledgements We thank the anonymous referees for their constructive comments as this helped in improving the quality of the paper.

Declarations

Conflict of interest The authors declare that they have no conflict of interest.

Appendix

A Asymptotic expansion of the total field

The ansatz representing the asymptotic expansion of the total field η for the Neumann boundary value problem used in the present paper is given by Melrose and Taylor in [45]. However, the authors did not present all the mathematical steps needed in its derivation. In this section, we provide the missing details of this analysis.

Let $K \subset \mathbb{R}^{n+1}$ be a compact strictly convex obstacle such that $B = \partial K \subset \mathbb{R}^{n+1}$ is a smooth hyper-surface, and consider the Neumann-to-Dirichlet operator

$$N^{-1} : \mathcal{E}'(\mathbb{R} \times B) \ni f(t,x) \mapsto v(t,x)|_{\mathbb{R}\times B} \in \mathcal{D}'(\mathbb{R} \times B) \tag{57}$$

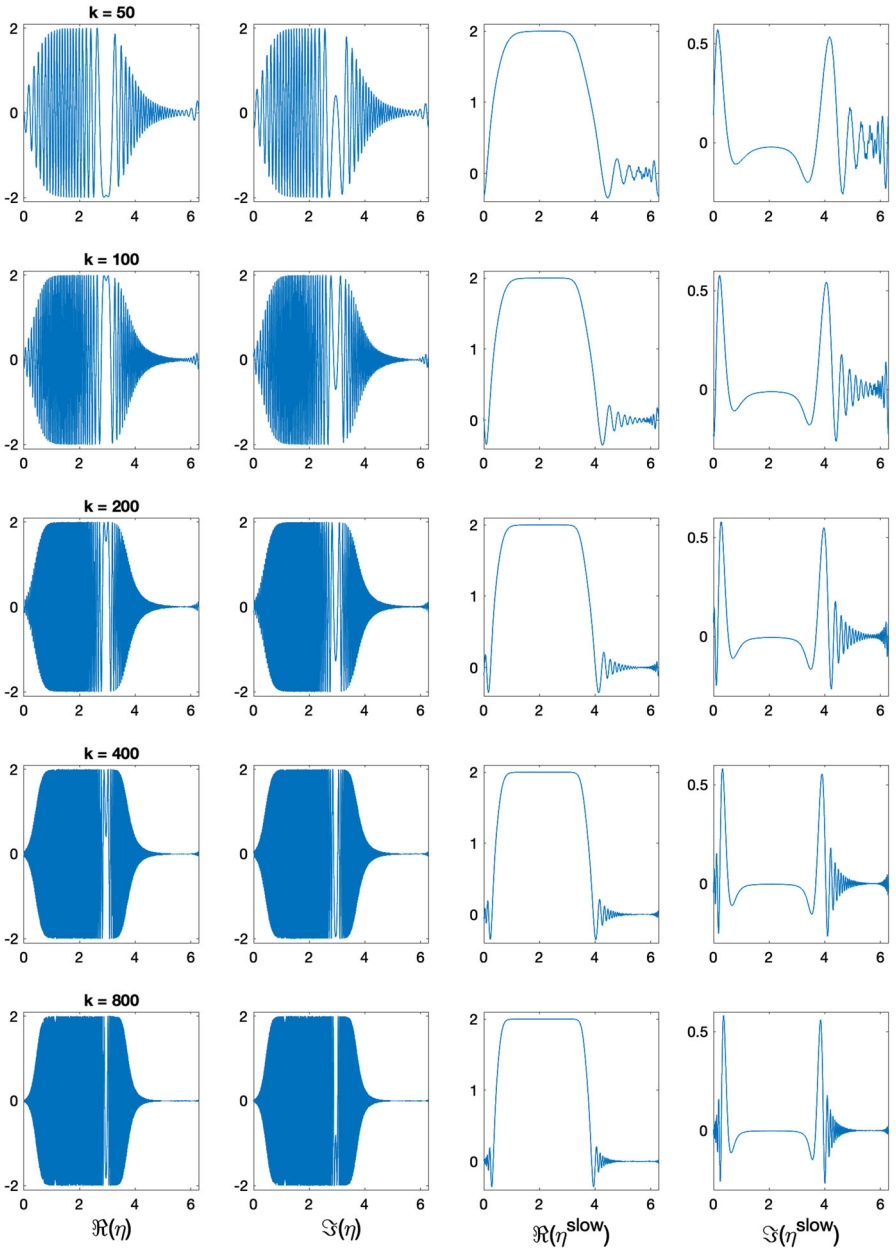

Fig. 8 Real (first column) and imaginary (second column) parts of η, and those of η^{slow} (columns three and four) associated with the elliptical scatterer in Fig. 5 for $k = 50, 100, 200, 400, 800$

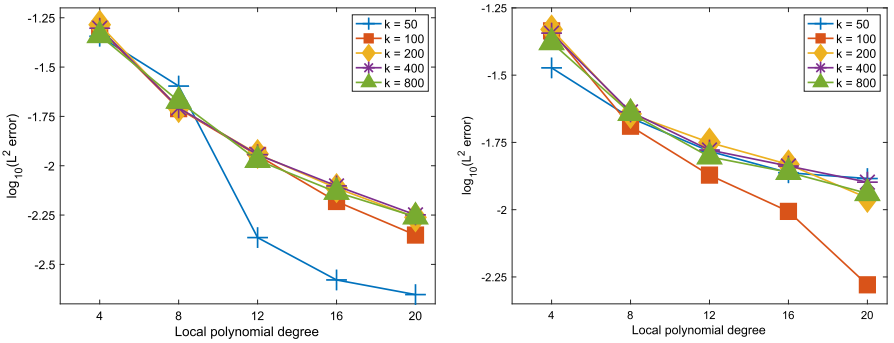

(a) Unit circle **(b)** Ellipse

Fig. 9 Local polynomial degree versus $\log_{10}(L^2$ error) for the unit circle (left) and the ellipse (right) for $k = 50, 100, 200, 400, 800$

where $\mathcal{D}'(B \times \mathbb{R})$ and $\mathcal{E}'(\mathbb{R} \times B)$ are the spaces of distributions and compactly supported distributions respectively, and v is the solution to the wave problem

$$\begin{cases} (\partial_{tt} - \Delta)v(t,x) = 0 & \text{in } \mathbb{R} \times \Omega, \\ \partial_\nu v(t,x)|_{\mathbb{R}\times B} = f(t,x) & \text{on } \mathbb{R} \times B, \end{cases} \tag{58}$$

wherein $\Omega = \mathbb{R}^{n+1} \setminus K$ is the exterior domain, and ν is the outward unit normal.

In what follows, for an incident field $v^i(t,x) = \delta(t - \alpha \cdot x)$ (δ is the Dirac function) with direction $\alpha \in \mathcal{S}^n$, we denote the solution of the wave problem (58) associated with $f(t,x) = (\alpha \cdot \nu(x))\partial_t v^i(t,x)$ by v. In this case, the total field $v^t := v + v^i$ can be expressed on the boundary as [45,p.296]

$$v^t(t,x)|_{\mathbb{R}\times B} = (I + N^{-1}(\alpha \cdot \nu(x))\partial_t)\delta(t - \alpha \cdot x) \tag{59}$$

where I is the identity operator. Using the same notation and procedure in [45], we define the *Kirchhoff operator* (see [45,Equation 8.26])

$$Q_N : \mathcal{E}'(\mathcal{S}^n \times \mathbb{R}) \ni v(t,x) \mapsto (I + N^{-1}(\alpha \cdot \nu(x))\partial_t)Fv(t,x) \in \mathcal{D}'(B \times \mathbb{R})$$

where F is the Fourier integral operator [41,Equation 9]

$$Fv(t,x) := \int_{\mathbb{R}\times\mathcal{S}^n} \kappa_F(t - s, w, x)v(s,\alpha)dsd\alpha \tag{60}$$

with kernel $\kappa_F(t,\alpha,x) := \delta(t - \alpha \cdot x)$.

As shown in [45], the asymptotic behavior of the total field η is determined by the kernel κ_{Q_N} of the Kirchhoff operator Q_N.

Lemma 6 *[45,Lemma 9.1] The asymptotic behavior as $k \to \pm\infty$ of the total field $\eta(\alpha, k, x)$ obtained by inverse Fourier transformation of the kernel $\kappa_{Q_N}(\alpha, t, x)$*

$$\eta(\alpha, x, k) = \int e^{itk} \kappa_{Q_N}(\alpha, t, x) dt \tag{61}$$

is determined by the singularities of the kernel κ_{Q_N} modulo rapidly decreasing terms.

The main goal is therefore the study of the kernel κ_{Q_N}. To this end, one first utilizes the general theory of *Fourier integral operators with folding canonical relations* [45,§5 and §6] to decompose the operator Q_N. In what follows, we use the notation in [45] except that $OPS^{\theta}_{\xi,\zeta}$ denotes the collection of pseudodifferential operators with symbols in the Hörmander class $S^{\theta}_{\xi,\zeta}$, and we write OPS^{θ} for $OPS^{\theta}_{1,0}$.

Theorem 6 *[45,Theorem 8.30] The Kirchhoff operator Q_N can be expressed as*

$$Q_N = J_1 D \mathcal{A}^{-1} J_2 \tag{62}$$

where J_1 and J_2 are elliptic Fourier integral operators of order zero, $D \in OPS^{-\frac{n}{2}-\frac{1}{6}}_{\frac{1}{3},0}$ has an asymptotic expansion

$$D \sim \sum_{r \in \mathbb{Z}_+,\, \ell \in -\mathbb{N}} A_{r,\ell} \Phi^{r,\ell} \tag{63}$$

with $A_{r,\ell} \in S^{-\frac{n}{2}-\frac{\ell}{3}-\frac{r}{3}+(\ell+1)_-}_{cl}$ and $\Phi^{r,\ell}(k^{-\frac{1}{3}}\xi_1) \in S^{(\frac{\ell}{3}-\frac{2r}{3})_+}_{\frac{1}{3},0}(\mathbb{R})$ (see [44,p.11-12]) so that

$$Dv(t,x) \sim \sum_{r \in \mathbb{Z}_+,\, \ell \in -\mathbb{N}} \int e^{i(x-y)\cdot\xi + i(t-t')k} a_{r,\ell}(t,x,k,\xi) \Phi^{r,\ell}(k^{-\frac{1}{3}}\xi_1) v(t',y) dt' dy dk d\xi \tag{64}$$

where (k, ξ) are variables dual to (t, x), and $a_{r,\ell} \in S^{-\frac{n}{2}-\frac{r}{3}-\frac{\ell}{3}+(\ell+1)_-}_{1,0}$ admits an asymptotic expansion

$$a_{r,\ell}(t,x,k,\xi) \sim \sum_{q \in \mathbb{Z}_+} k^{-\frac{n}{2}-q-\frac{r}{3}-\frac{\ell}{3}+(\ell+1)_-} a_{q,r,\ell}(t,x,\xi) \tag{65}$$

wherein $a_{q,r,\ell}$ are C^∞ functions uniformly bounded together with all their derivatives (cf. [42,Definition 2.5.6]), and $\mathcal{A}^{-1}$ is the convolution operator defined by Fourier transformation as [45,Equation 1.36]

$$\widehat{\mathcal{A}^{-1} v(t,x)}(\xi) = \frac{\hat{v}(\xi)}{A_+(k^{-\frac{1}{3}}\xi_1)}$$

where $A_+(z) := Ai(e^{\frac{2\pi i}{3}} z)$ *and* Ai *is the Airy function [43].*

The Fourier integral operator J_2 is given by

$$\begin{aligned} J_2 :&\mathcal{E}'(\mathbb{R}\times\mathcal{S}^n) \to \mathcal{D}'(\mathbb{R}\times\mathbb{R}^n)\\ :&v(s,\alpha) \mapsto (J_2 v)(t',y) = \int e^{i(y-\alpha)\cdot\xi - i(t'-s)k} a_{J_2}(s,\alpha,t',y) v(s,\alpha) ds d\alpha dk d\xi \end{aligned}$$

where $a_{J_2} \in S^0_{1,0}$ (a_{J_2} does not depend on ξ and k because it is a symbol of order 0). Applying the Dirac function at the base point $(0,\bar{\alpha})$ (see [41, 45]) yields

$$\begin{aligned} (J_2\delta_{(0,\bar{\alpha})})(t',y) &= \int e^{i(y-\alpha)\cdot\xi - i(t'-s)k} a_{J_2}(s,\alpha,t',y)\delta_{(0,\bar{\alpha})}(s,\alpha) ds d\alpha dk d\xi\\ &= \int e^{i(y-\bar{\alpha})\cdot\xi - it'k} a_{J_2}(\bar{\alpha},t',y) dk d\xi\\ &= \int e^{i(y-\bar{\alpha})\cdot\xi - it'k} a_{J_2}(\bar{\alpha},t',y)\widehat{\delta_0}(k,\xi) dk d\xi = (P\delta_0)(t',y) \end{aligned} \tag{66}$$

where the operator $P \in OPS^{-\frac{n}{2}+\frac{1}{6}}$ is specified by

$$(Pv)(t',y) := \int e^{i(y-\bar{\alpha})\cdot\xi - it'k} a_{J_2}(\bar{\alpha},y,t')\widehat{v}(k,\xi) dk d\xi.$$

Accordingly, use of (66) in (62) implies

$$Q_N(\delta_{(0,\bar{\alpha})}(t,x)) = J_1 D\mathcal{A}^{-1} J_2(\delta_{(0,\bar{\alpha})}(t,x)) = J_1 D\mathcal{A}^{-1} P(\delta_0(t,x)). \tag{67}$$

Finally, since $P\delta_0 = P^{\#}\delta_0 \mod OPS^{-\infty}$ and $P^{\#}$ commutes with $\mathcal{A}^{-1}$ [45,p.295], (67) can be rewritten as

$$Q_N(\delta_{(0,\bar{\alpha})}(t,x)) = J_1 DP^{\#}\mathcal{A}^{-1}(\delta_0(t,x)) \tag{68}$$

modulo rapidly decreasing terms.

In what follows, we briefly explain how representation (68) can be used to express the amplitude associated with the kernel κ_N as an asymptotic series of oscillatory integrals each of which is amenable to an application of the stationary phase method [28].

To this end, we first use (63) to deduce for the composition $DP^{\#}$ of the pseudo-differential operators D and $P^{\#}$

$$DP^{\#}v(t,x) \sim \sum_{\substack{r\in\mathbb{Z}_+\\ \ell\in-\mathbb{N}}} \int e^{i(x-y)\cdot\xi - i(t-t')k} a_{r,\ell}(t,x,k,\xi)\Phi^{r,\ell}(k^{-\frac{1}{3}}\xi_1) P^{\#}v(t',y) dt' dy dk d\xi \tag{69}$$

with

$$P^{\#}v(t',y) := \int e^{i(y-\bar{\alpha})\cdot\eta+it'\tau}\, p^{\#}(\bar{\alpha},t',y)\widehat{v}(\tau,\eta)d\tau d\eta$$
$$= \int e^{i(y-z-\bar{\alpha})\cdot\eta+i(t'-t'')\tau}\, p^{\#}(\bar{\alpha},t',y)v(t'',z)dt''dzd\tau d\eta \qquad (70)$$

where $p^{\#} \in S^0_{1,0}$, and (τ,η) is the dual variable to (t',y). Using (70) in (69), we therefore get

$$DP^{\#}v(t,x) \sim \sum_{\substack{r\in\mathbb{Z}_+\\ \ell\in-\mathbb{N}}} \int e^{i(x-z)\cdot\xi+(t-t'')k-i\bar{\alpha}\cdot\xi} b_{r,\ell}(\bar{\alpha},t,x,t'',z,k,\xi)$$
$$\Phi^{r,\ell}(k^{-\frac{1}{3}}\xi_1)v(t'',z)dt''dzdkd\xi \qquad (71)$$

with

$$b_{r,\ell}(\bar{\alpha},t,x,t'',z,k,\xi) := \int e^{i(y-z)\cdot(\eta-\xi)+i(t'-t'')(\tau-k)-i\bar{\alpha}\cdot(\eta-\xi)}$$
$$a_{r,\ell}(x,t,\xi,k)p^{\#}(\bar{\alpha},t',y)dt'dyd\tau d\eta.$$

As for the composition of the operator $DP^{\#}$ with the Fourier integral operator J_1 appearing in (62), let us first note that

$$J_1 : \mathcal{D}'(\mathbb{R}\times\mathbb{R}^n) \to \mathcal{D}'(\mathbb{R}\times B)$$
$$: v(t',y) \mapsto J_1v(t,x) = \int e^{i\psi_1(x,\tau,\eta)+i\tau(t-t')-iy\cdot\eta} a_{J_1}(x,t',y)v(t',y)dt'dyd\tau d\eta \qquad (72)$$

where (τ,η) are variables dual to (t,x), $a_{J_1} \in S^0_{1,0}$, and the phase function ψ_1 is defined in a neighborhood of the base point as [45,Equations 7.11 and 7.13]

$$\psi_1(x,\tau,\eta) = -\frac{|\eta'|^2}{2\tau} - \frac{|x'|^2\tau}{2} - \begin{cases} \frac{3}{2}(-\eta_1\tau^{-\frac{1}{3}})^{\frac{3}{2}}\operatorname{sgn}(\alpha\cdot\nu(x)), & \text{if } \alpha\cdot\nu(x)\neq 0,\\ 0, & \text{otherwise.}\end{cases} \qquad (73)$$

In (73), we have used the notation $x' = (x_2,\dots,x_n)$ for $x = (x_1,\dots,x_n) \in B$ and similarly for $\eta\in\mathbb{R}^n$. Combining (71) with (72), we obtain

$$J_1DP^{\#}v(t,x) \sim \sum_{\substack{r\in\mathbb{Z}_+\\ \ell\in-\mathbb{N}}} \int e^{i\psi_1(x,\tau,\eta)+i\tau(t-t')-iy\cdot\eta} a_{J_1}(x,t',y)\Big[\int e^{i(y-z)\xi+i(t'-t'')k-i\bar{\alpha}\cdot\xi}$$
$$b_{r,\ell}(\bar{\alpha},t',y,t'',z,k,\xi)\Phi^{r,\ell}(k^{-\frac{1}{3}}\xi_1)v(t'',z)dt''dzdkd\xi\Big]dt'dyd\tau d\eta,$$

and we rewrite this as

$$J_1 DP^{\#} v(t,x) \sim \sum_{\substack{r\in\mathbb{Z}_+\\ \ell\in-\mathbb{N}}} \int e^{i\psi_1(x,k,\xi)-i\bar{\alpha}\cdot\xi-itk-iz\xi-it''k} q_{N_{r,\ell}}(\bar{\alpha},x,t'',z,k,\xi)\Phi^{r,\ell}(k^{-\frac{1}{3}}\xi_1)v(t'',z)dt''dzdkd\xi \tag{74}$$

where

$$\begin{aligned} q_{N_{r,\ell}}(\bar{\alpha},x,t'',z,k,\xi) &:= a_{J_1}\#b_{r,\ell}(\bar{\alpha},x,t'',z,k,\xi)\\ &= \int e^{i\psi_1(x,\tau,\eta)-i\psi_1(x,k,\xi)+i(k-\tau)(t'-t)+i(\xi-\eta)\cdot y}\\ &\quad a_{J_1}(x,t',y)b_{r,\ell}(\bar{\alpha},t',y,t'',z,k,\xi)dt'dyd\tau d\eta. \end{aligned}$$

In light of (68), substituting [45,p.295]

$$\mathcal{A}^{-1}\delta_0(t'',z) = \int e^{i\xi\cdot z+ikt''}\frac{1}{A_+(k^{-\frac{1}{3}}\xi_1)}dkd\xi \tag{75}$$

for v in (74), we get

$$\begin{aligned} Q_N\delta_{(0,\bar{\alpha})}(t,x) &\sim \sum_{\substack{r\in\mathbb{Z}_+\\ \ell\in-\mathbb{N}}} \int e^{i\psi_1(x,k,\xi)-i\bar{\alpha}\cdot\xi-itk-iz\cdot\xi-it''k} q_{N_{r,\ell}}(\bar{\alpha},x,t'',z,k,\xi)\\ &\quad \Phi^{r,\ell}(k^{-\frac{1}{3}}\xi_1)\mathcal{A}^{-1}\delta_0(t'',z)dt''dzdkd\xi\\ &\sim \sum_{\substack{r\in\mathbb{Z}_+\\ \ell\in-\mathbb{N}}} \int e^{i\psi_1(x,k,\xi)-i\bar{\alpha}\cdot\xi-itk} q_{N_{r,\ell}}(\bar{\alpha},x,k,\xi)\frac{\Phi^{r,\ell}(k^{-\frac{1}{3}}\xi_1)}{A_+(k^{-\frac{1}{3}}\xi_1)}dkd\xi \end{aligned} \tag{76}$$

where $q_{N_{r,\ell}}(\bar{\alpha},x,k,\xi) := a_J\#b_{r,\ell}(\bar{\alpha},x,k,\xi)$.

For the kernel κ_{Q_N}, we accordingly have

$$\kappa_{Q_N}(\alpha,t,x) \sim \sum_{\substack{r\in\mathbb{Z}_+\\ \ell\in-\mathbb{N}}} \int e^{i\psi_1(x,k,\xi)-i\bar{\alpha}\cdot\xi-itk} q_{N_{r,\ell}}(\bar{\alpha},x,k,\xi)\frac{\Phi^{r,\ell}(k^{-\frac{1}{3}}\xi_1)}{A_+(k^{-\frac{1}{3}}\xi_1)}dkd\xi$$

and, in virtue of Lemma 6, we deduce (see [45,p.298])

$$\eta(\alpha,x,k) \sim \sum_{\substack{r\in\mathbb{Z}_+\\ \ell\in-\mathbb{N}}} \int e^{i\psi_1(x,\xi,k)-i\bar{\alpha}\cdot\xi} q_{N_{r,\ell}}(\bar{\alpha},x,k,\xi)\frac{\Phi^{r,\ell}(k^{-\frac{1}{3}}\xi_1)}{A_+(k^{-\frac{1}{3}}\xi_1)}d\xi. \tag{77}$$

Making the change of variable $\xi = k\zeta$ in (77), we therefore find [45,p.298]

$$\eta(\alpha, x, k) \sim \sum_{\substack{r\in\mathbb{Z}_+\\ \ell\in-\mathbb{N}}} \int e^{ik\psi_2(\alpha,x,\zeta)} q_{N_{r,\ell}}(\bar{\alpha}, x, k, \zeta) \frac{\Phi^{r,\ell}(k^{\frac{2}{3}}\zeta_1)}{A_+(k^{\frac{2}{3}}\zeta_1)} d\zeta \tag{78}$$

where $\psi_2(\alpha, x, \zeta) = \psi_1(x, 1, \zeta) - \bar{\alpha}\cdot\zeta$, and with a slight abuse of notation we have written $q_{N_{r,\ell}}(\bar{\alpha}, x, k, \zeta)$ for $k^n q_{N_{r,\ell}}(\bar{\alpha}, x, k, \zeta)$. In this case, $q_{N_{r,\ell}}$ is a symbol of order $\frac{n}{2} + \frac{1}{6} - \frac{r}{3} - \frac{\ell}{3} + (\ell+1)_-$ so that

$$q_{N_{r,\ell}}(\bar{\alpha}, x, k, \zeta) \sim \sum_{q\in\mathbb{Z}_+} k^{\frac{n}{2}+\frac{1}{6}-q-\frac{r}{3}-\frac{\ell}{3}+(\ell+1)_-} q_{N_{q,r,\ell}}(\bar{\alpha}, x, \zeta). \tag{79}$$

Using (79) in (78), we arrive at

$$\eta(\alpha, x, k) \sim \sum_{\substack{q,r\in\mathbb{Z}_+\\ \ell\in-\mathbb{N}}} k^{\frac{n}{2}+\frac{1}{6}-q-\frac{r}{3}-\frac{\ell}{3}+(\ell+1)_-} \int e^{ik\psi_2(\alpha,x,\zeta)} q_{N_{q,r,\ell}}(\bar{\alpha}, x, \zeta) \frac{\Phi^{r,\ell}(k^{\frac{2}{3}}\zeta_1)}{A_+(k^{\frac{2}{3}}\zeta_1)} d\zeta. \tag{80}$$

In order to further simplify (80), we introduce the function

$$\Psi^{r,\ell}(\tau) := e^{-\frac{i\tau^3}{3}} \int \frac{\Phi^{r,\ell}(s)}{A_+(s)} e^{-is\tau} ds. \tag{81}$$

The symbolic behavior of $\Psi^{r,\ell}$ is as follows.

Lemma 7 *[45,Lemma 9.34] The function $\Psi^{r,\ell}$ defined in (81) belongs to $S^{1+\ell-2r}(\mathbb{R})$, admits an asymptotic expansion*

$$\Psi^{r,\ell}(\tau) \sim \sum_{j\in\mathbb{Z}_+} \alpha_{r,\ell,j} \tau^{1+\ell-2r-3j} \tag{82}$$

as $\tau \to +\infty$, and is rapidly decreasing in the sense of Schwarz as $\tau \to -\infty$.

Rewriting (81) as

$$e^{\frac{i\tau^3}{3}} \Psi^{r,\ell}(\tau) = \int \frac{\Phi^{r,\ell}(s)}{A_+(s)} e^{-is\tau} ds = \widehat{\left(\frac{\Phi^{r,\ell}}{A_+}\right)}(\tau),$$

and using $\mathcal{F}^{-1}$ to denote the inverse Fourier transform, we obtain

$$\begin{aligned} \frac{\Phi^{r,\ell}(k^{\frac{2}{3}}\zeta_1)}{A_+(k^{\frac{2}{3}}\zeta_1)} &= \mathcal{F}^{-1}\Big(\widehat{\Big(\frac{\Phi^{r,\ell}}{A_+}\Big)}(\tau)\Big)(k^{\frac{2}{3}}\zeta_1) = \mathcal{F}^{-1}\Big(e^{\frac{i\tau^3}{3}}\Psi^{r,\ell}(\tau)\Big)(k^{\frac{2}{3}}\zeta_1) \\ &= \int e^{ik^{\frac{2}{3}}\zeta_1\tau} e^{\frac{i\tau^3}{3}} \Psi^{r,\ell}(\tau) d\tau = k^{\frac{1}{3}} \int e^{ik\zeta_1 t + ik\frac{t^3}{3}} \Psi^{r,\ell}(k^{\frac{1}{3}}t) dt. \end{aligned} \tag{83}$$

Using (83) in (80), we finally conclude

$$\eta(\alpha, x, k) \sim k^{\frac{1}{3}} \sum_{\substack{q,r\in\mathbb{Z}_+ \\ \ell\in-\mathbb{N}}} k^{\frac{n}{2}+\frac{1}{6}-q-\frac{r}{3}-\frac{\ell}{3}+(\ell+1)-} I_{q,r,\ell}(\alpha, x, k) \tag{84}$$

where

$$I_{q,r,\ell}(\alpha, x, k) := \int e^{ik\psi_3(\zeta,t)} q_{N_{q,r,\ell}}(\bar{\alpha}, x, \zeta)\Psi^{r,\ell}(k^{\frac{1}{3}}t)d\zeta\, dt \tag{85}$$

with the phase function given by

$$\psi_3(\zeta, t) := \psi_2(\alpha, x, \zeta) + t\zeta_1 + \frac{t^3}{3}. \tag{86}$$

As shown in [45], the integrals $I_{q,r,\ell}(\alpha, k, x)$ can be treated using the stationary phase method which results in

$$I_{q,r,\ell}(\alpha, x, k) \sim k^{-\frac{1}{3}} \sum_{p\in\mathbb{Z}_+} k^{-\frac{n+1}{2}-\frac{2p}{3}} a_{p,q,r,\ell}(\alpha, x)\, (\Psi^{r,\ell})^{(p)}(k^{\frac{1}{3}} Z(\alpha, x))\, e^{ik\alpha\cdot x}, \tag{87}$$

and this leads into the following for the envelope $\eta^{\text{slow}}(\alpha, k, x) = e^{-ik\alpha\cdot x}\eta(\alpha, k, x)$.

Theorem 7 *[45,Theorem 9.36] In a vicinity of the shadow boundary $\{x \in B : \alpha \cdot \nu(x) = 0\}$, $\eta^{\text{slow}}(\alpha, k, x)$ belongs to the Hörmander class $S^0_{\frac{2}{3},\frac{1}{3}}$ and admits an asymptotic expansion*

$$\eta^{\text{slow}}(\alpha, x, k) \sim \sum_{\substack{q,p,r\in\mathbb{Z}_+ \\ \ell\in-\mathbb{N}}} a_{p,q,r,\ell}(\alpha, x, k) \tag{88}$$

with

$$a_{p,q,r,\ell}(\alpha, x, k) := k^{-\frac{1}{3}-\frac{2p}{3}-q-\frac{r}{3}-\frac{\ell}{3}+(\ell+1)-} b_{p,q,r,\ell}(\alpha, x)\, (\Psi^{r,\ell})^{(p)}(k^{\frac{1}{3}} Z(\alpha, x))$$

where $b_{p,q,r,\ell}$ are complex-valued C^∞ functions, Z is a real-valued C^∞ function that is positive on the illuminated region $\{x \in B : \alpha \cdot \nu(x) < 0\}$, negative on the shadow region $\{x \in B : \alpha \cdot \nu(x) > 0\}$, and that vanishes precisely to first order at the shadow boundary.

Under certain assumptions, Theorem 7 is in fact valid over the entire boundary B. This is given in the next theorem where we use the notation $B^\epsilon_{\gtrless} = \{x \in B : \alpha \cdot \nu(x) \gtrless \epsilon\}$.

Theorem 8 *Assume there exists $\epsilon \in (0,1)$ such that on $B^{\epsilon}_{<}$ the envelope η^{slow} belongs to $S^0_{1,0}(B^{\epsilon}_{<} \times (0,\infty))$ and admits an asymptotic expansion*

$$\eta^{\text{slow}}(\alpha, x, k) \sim \sum_{j \in \mathbb{Z}_+} k^{-j}\, a_j(\alpha, x), \quad \text{as } k \to \infty, \tag{89}$$

and it is rapidly decreasing in the sense of Schwarz on $B^{\epsilon}_{>}$ as $k \to -\infty$. Then $\eta^{\text{slow}} \in S^0_{\frac{1}{3},\frac{1}{3}}(B \times (0,\infty))$ and the asymptotic expansion (88) is valid over the entire boundary B.

The proof of Theorem 8 follows the same lines as in the proof of [23,Corollary 5.3] (see also [27,Theorem 3.1 and Corollary 2.1]) and is based on the standard *matching of asymptotic expansions technique* (see e.g. [23] and the references therein). The expansion (89) related to Neumann problem is similar to the one given in [45,Equation 1.15] for the Dirichlet case. Furthermore, using the references provided in [23] (see the proof of Corollary 5.3) we can deduce that, for the two-dimensional Neumann boundary value problem, η^{slow} decays exponentially in $B^{\epsilon}_{>}$ as $k \to -\infty$ which implies the assumption of its rapid decay in the sense of Schwarz in Theorem 8.

B Auxiliary results

Here we provide auxiliary results used in the proofs.

Lemma 8 *[24,Lemma 14] Let $a(s,k) = k^{\theta}\, b(s)\, \varphi(k^{\omega} \Upsilon(s))$ where b, φ and Υ are smooth functions, b and Υ are periodic, and $\theta \in \mathbb{R}\backslash\mathbb{N}$ and $\omega \in \mathbb{R}\backslash\mathbb{Z}_+$. Then*

$$|D_s^n D_k^m\, a(s,k)| \lesssim k^{\theta - m} \sum_{j=0}^{n+m} k^{j\omega} |\varphi^{(j)}(k^{\omega}\Upsilon(s))|$$

for all $n, m \in \mathbb{Z}_+$ and all $k > 0$.

Theorem 9 *[47,Corollary 3.12] Given a function $f \in C^{\infty}([a,b])$ and $n \in \mathbb{Z}_+$, there exists a constant $C_n > 0$ such that*

$$\inf_{p \in \mathbb{P}_d} \|f - p\|_{L^2[(a,b)]} \leq C_n \left[\int_a^b \left| D^n f(s) \right|^2 (s-a)^n\, (b-s)^n\, ds \right]^{\frac{1}{2}} d^{-n}$$

for all $d \in \mathbb{N}$ with $d + 1 \geq n$.

Lemma 9 *[24,Lemma 14] Suppose that either $[\alpha, \beta] \subseteq [t_1, t_2] \subseteq (c, d)$ or $[\alpha, \beta] \cap (t_1, t_2) = \varnothing$ and $[c, d] \subseteq (t_1, t_2)$. Then, for any $a, b \in \mathbb{R}$, $n \in \mathbb{N} \cup \{0\}$, $m \in \mathbb{N}$, there holds*

$$\int_{\alpha}^{\beta} \frac{(s-a)^n\, (b-s)^n}{(s-c)^m\, (d-s)^m}\, ds$$

$$= \sum_{\substack{0\le p,q\le n\\ 1\le j\le m}} \binom{2m-j-1}{m-j}\binom{n}{p}\binom{n}{q}\frac{(-1)^n\,\mathcal{F}(\alpha,\beta;a,b;c,d;n,p,q;j)}{(d-c)^{2m-j}}.$$

Here we have

$$\mathcal{F}(\alpha,\beta;a,b;c,d;n,p,q;j) = (c-a)^p\,(c-b)^q\log\left(\frac{\beta-c}{\alpha-c}\right) + (a-d)^p\,(b-d)^q\log\left(\frac{d-\alpha}{d-\beta}\right)$$

when $2n-(p+q+j)=-1$, *and*

$$\begin{aligned}&\mathcal{F}(\alpha,\beta;a,b;c,d;n,p,q;j)\\ &= \frac{(c-a)^p\,(c-b)^q}{2n-(p+q+j)+1}\left[(\beta-c)^{2n-(p+q+j)+1}-(\alpha-c)^{2n-(p+q+j)+1}\right]\\ &+ \frac{(a-d)^p\,(b-d)^q}{2n-(p+q+j)+1}\left[(d-\alpha)^{2n-(p+q+j)+1}-(d-\beta)^{2n-(p+q+j)+1}\right]\end{aligned}$$

when $2n-(p+q+j)\neq -1$.

References

1. Abramowitz, M., Stegun, I.A.: Handbook of mathematical functions with formulas, graphs, and mathematical tables, National Bureau of Standards Applied Mathematics Series, vol. 55. U.S. Government Printing Office, Washington, D.C, For sale by the Superintendent of Documents (1964)
2. Amini, S., Profit, A.: Multi-level fast multipole solution of the scattering problem. Eng. Anal. Bound. Elem. **27**(5), 547–564 (2003)
3. Anand, A., Boubendir, Y., Ecevit, F., Reitich, F.: Analysis of multiple scattering iterations for high-frequency scattering problems. II. The three-dimensional scalar case. Numer. Math. **114**(3), 373–427 (2010)
4. Banjai, L., Hackbusch, W.: Hierarchical matrix techniques for low- and high-frequency Helmholtz problems. IMA J. Numer. Anal. **28**(1), 46–79 (2008)
5. Boffi, D.: Finite element approximation of eigenvalue problems. Acta Numer. **19**, 1–120 (2010)
6. Boubendir, Y., Turc, C.: Wave-number estimates for regularized combined field boundary integral operators in acoustic scattering problems with Neumann boundary conditions. IMA J. Numer. Anal. **33**(4), 1176–1225 (2013)
7. Bruno, O., Geuzaine, C., Reitich, F.: On the $O(1)$ solution of multiple-scattering problems. IEEE Trans. Magn. **41**(5), 1488–1491 (2005)
8. Bruno, O.P., Domínguez, V., Sayas, F.J.: Convergence analysis of a high-order Nyström integral-equation method for surface scattering problems. Numer. Math. **124**(4), 603–645 (2013)
9. Bruno, O.P., Geuzaine, C.A.: An $O(1)$ integration scheme for three-dimensional surface scattering problems. J. Comput. Appl. Math. **204**(2), 463–476 (2007)
10. Bruno, O..P., Geuzaine, C..A., Monro, J..A., Jr., Reitich, F.: Prescribed error tolerances within fixed computational times for scattering problems of arbitrarily high frequency: the convex case. Philos. Trans. R. Soc. Lond. Ser. A Math. Phys. Eng. Sci. **362**(1816), 629–645 (2004)
11. Bruno, O.P., Kunyansky, L.A.: A fast, high-order algorithm for the solution of surface scattering problems: basic implementation, tests, and applications. J. Comput. Phys. **169**(1), 80–110 (2001)
12. Céa, J.: Approximation variationnelle des problèmes aux limites. Ann. Inst. Fourier (Grenoble) **14**(fasc. 2), 345–444 (1964)

13. Chandler-Wilde, S.N., Graham, I.G.: Boundary integral methods in high frequency scattering. In: Highly oscillatory problems, London Math. Soc. Lecture Note Ser., vol. 366, pp. 154–193. Cambridge University Press, Cambridge (2009)
14. Chandler-Wilde, S.N., Graham, I.G., Langdon, S., Spence, E.A.: Numerical-asymptotic boundary integral methods in high-frequency acoustic scattering. Acta Numer. **21**, 89–305 (2012)
15. Chandler-Wilde, S.N., Hewett, D.P.: Wavenumber-explicit continuity and coercivity estimates in acoustic scattering by planar screens. Integr. Equa. Oper. Theory **82**(3), 423–449 (2015)
16. Chandler-Wilde, S.N., Hewett, D.P., Langdon, S., Twigger, A.: A high frequency boundary element method for scattering by a class of nonconvex obstacles. Numer. Math. **129**(4), 647–689 (2015)
17. Chandler-Wilde, S.N., Langdon, S.: A Galerkin boundary element method for high frequency scattering by convex polygons. SIAM J. Numer. Anal. **45**(2), 610–640 (2007)
18. Chandler-Wilde, S.N., Langdon, S., Mokgolele, M.: A high frequency boundary element method for scattering by convex polygons with impedance boundary conditions. Commun. Comput. Phys. **11**(2), 573–593 (2012)
19. Chandler-Wilde, S.N., Spence, E.A., Gibbs, A., Smyshlyaev, V.P.: High-frequency bounds for the Helmholtz equation under parabolic trapping and applications in numerical analysis. SIAM J. Math. Anal. **52**(1), 845–893 (2020)
20. Colton, D., Kress, R.: Inverse Acoustic and Electromagnetic Scattering Theory, Applied Mathematical Sciences, vol. 93. Springer, Berlin (1992)
21. Colton, D.L., Kress, R.: Integral Equation Methods in Scattering Theory. Pure and Applied Mathematics (New York). Wiley, New York (1983)
22. Davies, R.W., Morgan, K., Hassan, O.: A high order hybrid finite element method applied to the solution of electromagnetic wave scattering problems in the time domain. Comput. Mech. **44**(3), 321–331 (2009)
23. Domínguez, V., Graham, I.G., Smyshlyaev, V.P.: A hybrid numerical-asymptotic boundary integral method for high-frequency acoustic scattering. Numer. Math. **106**(3), 471–510 (2007)
24. Ecevit, F.: Frequency independent solvability of surface scattering problems. Turkish J. Math. **42**(2), 407–422 (2018)
25. Ecevit, F., Eruslu, H.H.: A Galerkin BEM for high-frequency scattering problems based on frequency-dependent changes of variables. IMA J. Numer. Anal. **39**(2), 893–923 (2019)
26. Ecevit, F., Özen, H.Ç.: Frequency-adapted Galerkin boundary element methods for convex scattering problems. Numer. Math. **135**(1), 27–71 (2017)
27. Ecevit, F., Reitich, F.: Analysis of multiple scattering iterations for high-frequency scattering problems. I. The two-dimensional case. Numer. Math. **114**(2), 271–354 (2009)
28. Fedoryuk, M.V.: The stationary phase method and pseudodifferential operators. Russ. Math. Surv. **26**(1), 65 (1971)
29. Galkowski, J.: Distribution of resonances in scattering by thin barriers. Mem. Am. Math. Soc. **259**(1248), ix+152 (2019)
30. Galkowski, J., Müller, E.H., Spence, E.A.: Wavenumber-explicit analysis for the Helmholtz h-BEM: error estimates and iteration counts for the Dirichlet problem. Numer. Math. **142**(2), 329–357 (2019)
31. Giladi, E., Keller, J.B.: An asymptotically derived boundary element method for the helmholtz equations. Appl. Comput. Electromagn. Soc. (2004)
32. Groth, S., Hewett, D., Langdon, S.: A hybrid numerical-asymptotic boundary element method for high frequency scattering by penetrable convex polygons. Wave Motion **78**, 32–53 (2018)
33. Groth, S.P., Hewett, D.P., Langdon, S.: Hybrid numerical-asymptotic approximation for high-frequency scattering by penetrable convex polygons. IMA J. Appl. Math. **80**(2), 324–353 (2013)
34. Hesthaven, J., Warburton, T.: High-order accurate methods for time-domain electromagnetics. CMES Comput. Model. Eng. Sci. **5**(5), 395–407 (2004)
35. Hewett, D.P.: Shadow boundary effects in hybrid numerical-asymptotic methods for high-frequency scattering. Eur. J. Appl. Math. **26**(5), 773–793 (2015)
36. Hewett, D.P., Langdon, S., Chandler-Wilde, S.N.: A frequency-independent boundary element method for scattering by two-dimensional screens and apertures. IMA J. Numer. Anal. **35**(4), 1698–1728 (2015)
37. Hewett, D.P., Langdon, S., Melenk, J.M.: A high frequency hp boundary element method for scattering by convex polygons. SIAM J. Numer. Anal. **51**(1), 629–653 (2013)
38. Huybrechs, D., Vandewalle, S.: A sparse discretization for integral equation formulations of high frequency scattering problems. SIAM J. Sci. Comput. **29**(6), 2305–2328 (2007)

39. Johnson, W.P.: The curious history of Faà di Bruno's formula. Am. Math. Monthly **109**(3), 217–234 (2002)
40. Langdon, S., Mokgolele, M., Chandler-Wilde, S.: High frequency scattering by convex curvilinear polygons. J. Comput. Appl. Math. **234**(6), 2020–2026 (2010)
41. Lazergui, S., Boubendir, Y.: Asymptotic expansions of the Helmholtz equation solutions using approximations of the Dirichlet to Neumann operator. J. Math. Anal. Appl. **456**(2), 767–786 (2017)
42. Martinez, A.: An Introduction to Semiclassical and Microlocal Analysis. Springer, New York (2002)
43. Melrose, R.B.: Local Fourier-Airy integral operators. Duke Math. J. **42**(4), 583–604 (1975)
44. Melrose, R.B.: Airy operators. Commun. Partial. Differ. Equ. **3**(1), 1–76 (1978)
45. Melrose, R.B., Taylor, M.E.: Near peak scattering and the corrected Kirchhoff approximation for a convex obstacle. Adv. Math. **55**(3), 242–315 (1985)
46. Namburu, R., Mark, E., Clarke, J.: Scalable electromagnetic simulation environment. CMES Comput. Model. Eng. Sci. **5**(5), 443–453 (2004)
47. Schwab, C.: *p*- and *hp*-Finite Element Methods. Numerical Mathematics and Scientific Computation. The Clarendon Press, Oxford University Press, New York (1998)
48. Sherer, S.E., Visbal, M.R.: Time-domain scattering simulations using a high-order overset-grid approach. In: Workshop on Computational Electromagnetics in Time-Domain, 2005. CEM-TD 2005., pp. 44–47 (2005)
49. Taflove, A., Hagness, S.C.: Computational electrodynamics: The finite-difference time-domain method, 2nd edn. Artech House Inc, Boston (2000)
50. Tong, M.S., Chew, W.C.: Multilevel fast multipole acceleration in the Nyström discretization of surface electromagnetic integral equations for composite objects. IEEE Trans. Antennas Propagat. **58**(10), 3411–3416 (2010)